AD-A061 943 PENNSYLVANIA STATE UNIV UNIVERSITY PARK APPLIED RESE--ETC F/G 20/11
THE EFFECTIVENESS OF SOME RECENT DAMPING TREATMENTS IN THE REDU--ETC(U)
AUG 78 R W THOMAS N00017-47-C-14189

UNCLASSIFIED TM-78-209 NL

1 OF
AD
A061 943

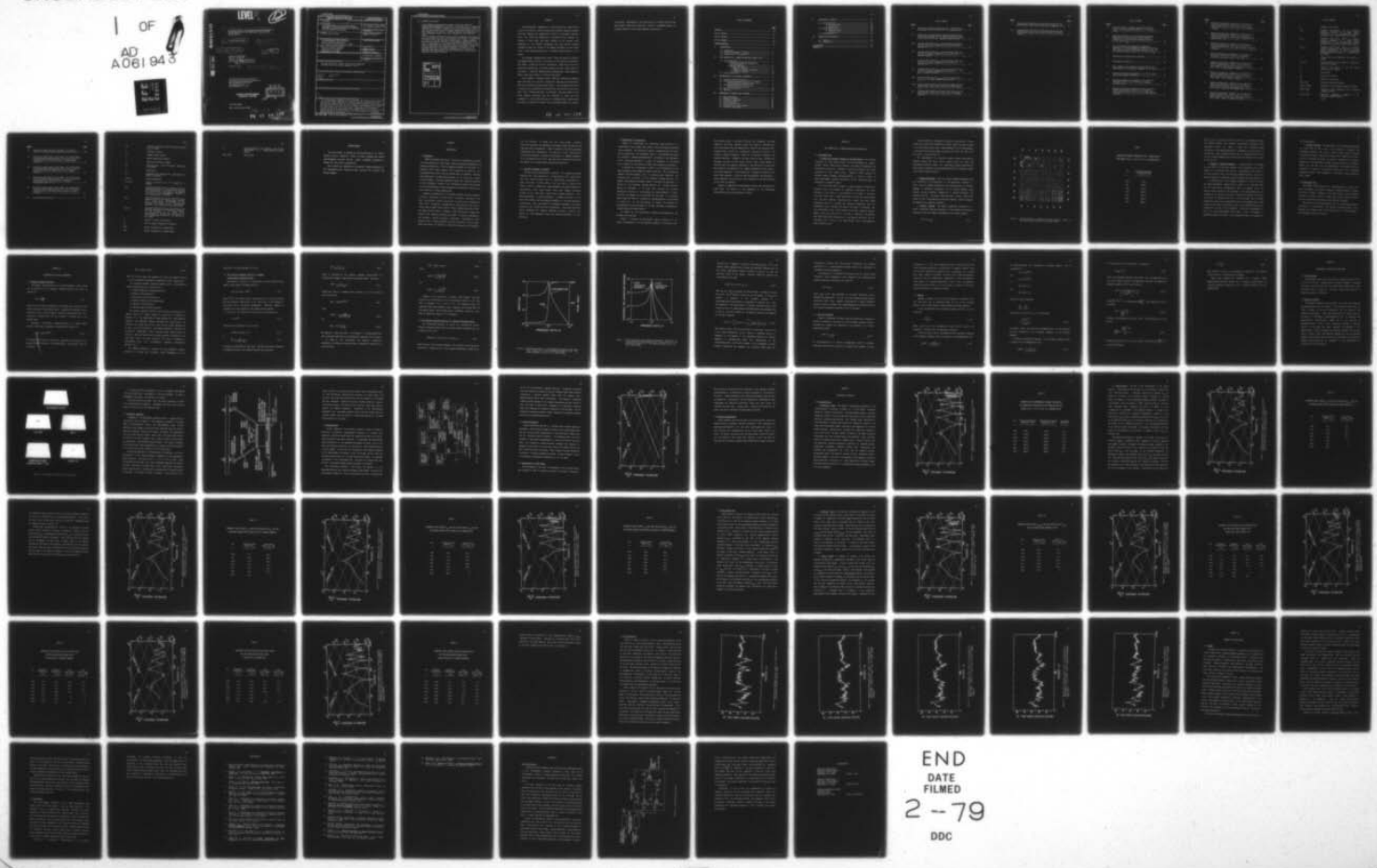

END
DATE
FILMED
2-79
DDC

61 94

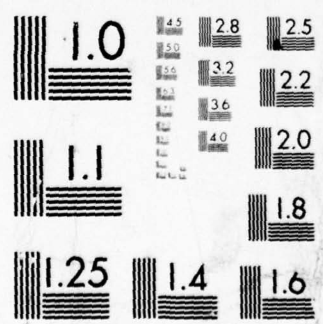

MICROCOPY RESOLUTION TEST CHART
NATIONAL BUREAU OF STANDARDS-1963-A

(12)

(6) THE EFFECTIVENESS OF SOME RECENT DAMPING TREATMENTS IN THE REDUCTION OF THE VIBRATION OF FLUID-LOADED FINITE PLATES.

(10) Richard Wells/Thomas

(11) 4 Aug 78

(14) TM-78-209

(12) 91 p.

Technical Memorandum
File No. TM 78-209
August 4, 1978
Contract No. (15) N00017-73-C-1418

Copy No. 5

(9) master's thesis,

The Pennsylvania State University
Institute for Science and Engineering
APPLIED RESEARCH LABORATORY
Post Office Box 30
~~State College~~, PA 16801
University Park

NAVY DEPARTMENT

NAVAL SEA SYSTEMS COMMAND

UNCLASSIFIED

SECURITY CLASSIFICATION OF THIS PAGE *(When Data Entered)*

REPORT DOCUMENTATION PAGE		READ INSTRUCTIONS BEFORE COMPLETING FORM
1. REPORT NUMBER TM 78-209	2. GOVT ACCESSION NO.	3. RECIPIENT'S CATALOG NUMBER
4. TITLE *(and Subtitle)* THE EFFECTIVENESS OF SOME RECENT DAMPING TREATMENTS IN THE REDUCTION OF THE VIBRATION OF FLUID-LOADED FINITE PLATES		5. TYPE OF REPORT & PERIOD COVERED M.S. Thesis, December 1978 6. PERFORMING ORG. REPORT NUMBER TM 78-209
7. AUTHOR(s) Richard Wells Thomas		8. CONTRACT OR GRANT NUMBER(s) N00017-73-C-1418
9. PERFORMING ORGANIZATION NAME AND ADDRESS The Pennsylvania State University Applied Research Laboratory P. O. Box 30, State College, PA 16801		10. PROGRAM ELEMENT, PROJECT, TASK AREA & WORK UNIT NUMBERS
11. CONTROLLING OFFICE NAME AND ADDRESS Naval Sea Systems Command Department of the Navy Washington, DC 20362		12. REPORT DATE August 4, 1978 13. NUMBER OF PAGES 89 pages & figures
14. MONITORING AGENCY NAME & ADDRESS*(if different from Controlling Office)*		15. SECURITY CLASS. *(of this report)* Unclassified, Unlimited 15a. DECLASSIFICATION/DOWNGRADING SCHEDULE

16. DISTRIBUTION STATEMENT *(of this Report)*

Approved for public release, distribution unlimited, per NSSC (Naval Sea Systems Command), 9/1/78

17. DISTRIBUTION STATEMENT *(of the abstract entered in Block 20, if different from Report)*

18. SUPPLEMENTARY NOTES

19. KEY WORDS *(Continue on reverse side if necessary and identify by block number)*

vibration
damping
plates
fluid loading
coating

20. ABSTRACT *(Continue on reverse side if necessary and identify by block number)*

The driving-point impedance of center-driven free square plates coated on one side by several commercially available damping treatments have been measured and compared with that of an uncoated, reference plate. The plates were subjected to two types of fluid loading: air loading of both sides, and water loading of the uncoated side. Comparison of the resonance frequencies and loss factors provided information about the effects of the damping treatments and the change in the fluid loading on the dynamic characteristics of the plates. (continued) - -

DD FORM 1 JAN 73 1473 EDITION OF 1 NOV 65 IS OBSOLETE

next page

UNCLASSIFIED

SECURITY CLASSIFICATION OF THIS PAGE *(When Data Entered)*

20. ABSTRACT (Continued)

Four damping treatments were tested. These were Epoxy 10, Embossed Foam Damping Sheet, and GP-1, all products of the Soundcoat Corporation, and LD400, a product of the Lord Corporation. Epoxy 10 and GP-1 were supplied as semi-fluids, which were troweled onto the upper surface of the plates. LD400 and Embossed Foam Damping Sheet were prehardened sheets, which were attached to the plates with epoxy.

Of the damping treatments tested, LD400 and Embossed Foam Damping Sheet were found to be the most effective in reducing the vibrations of both the air loaded and water loaded plates. These treatments were seen to cause an increase in the resonant frequencies of the plates. Measurements of the sound level in the direct field of the water loaded plates have shown that these two treatments caused the greatest reduction in the sound radiated by the plates. It is concluded that tile type damping treatments, such as LD400 and Embossed Foam Damping Sheet, are most effective in reducing plate vibrations and sound radiation.

ABSTRACT

The driving-point impedances of center-driven free square plates coated on one side by several commercially available damping treatments have been measured and compared with those of an uncoated reference plate. The plates were subjected to two types of fluid loading: air loading of both sides, and water loading of the uncoated side. Comparison of the resonant frequencies and loss factors provided information about the effects of the damping treatments and the change in the fluid loading conditions on the dynamic characteristics of the plates.

Four damping treatments were tested. These were Epoxy 10, Embossed Foam Damping Sheet, and GP-1, all products of the Soundcoat Corporation, and LD400, a product of the Lord Corporation. Epoxy 10 and GP-1 were supplied as semi-fluids, which were troweled onto the upper surface of the plates. LD400 and Emobossed Foam Damping Sheet were prehardened sheets, which were attach to the plates with epoxy.

Of the damping treatments tested, LD400 and Embossed Foam Damping Sheet were found to be the most effective in reducing the vibrations of both the air-loaded and water-loaded plates. These treatments were seen to cause the most significant increase in the loss factors of each plate mode. This increase was found to be greater than that caused by the fluid loading, indicating that the addition of these tile type treatments to the internal portions of a submerged body should reduce the energy available for transfer into the ambient medium as acoustic

sound waves. Measurements of the sound level in the direct field of the water-loaded plates have shown that these two treatments caused the greatest reduction in the sound radiated by the plates.

TABLE OF CONTENTS

LIST OF TABLES

LIST OF FIGURES

LIST OF SYMBOLS

B	frequency ratio (w/w_n)
$D_{f,a}$	Frequency Shift Factor: ratio of a measured resonant frequency of a coated plate, air-loaded, to the corresponding resonant frequency of the uncoated plate, air-loaded
$D_{f,w}$	Frequency Shift Factor: ratio of a measured resonant frequency of a coated plate, water-loaded, to the corresponding resonant frequency of the uncoated plate, water-loaded
$D_{f,w-a}$	Frequency Shift Factor: Ratio of a measured resonant frequency of the uncoated or a coated plate, water-loaded, to the corresponding measured resonant frequency of the same plate, air-loaded
f_o	total driving force amplitude impressed on a system
$f(x,y,z)$	external harmonic force exerted on a system per unit area or volume
G_n	effective loss factor of the n^{th} natural function q_n of a system
g	loss factor
g_m	material loss factor
g_r	radiation loss factor
$H(w)$, $H(B)$	frequency response functions
$\|H(w)\|$, $\|H(B)\|$	magnitude of the frequency response function
$H_R(w)$, $H_R(B)$	coincident (real) component of the frequency response function
$H_I(w)$, $H_I(B)$	quadrature (imaginary) component of the frequency response function
j	$\sqrt{-1}$

K_n	effective stiffness of the n^{th} natural function q_n of a system
k	stiffness constant
k^*	complex elastic modulus
L	linear differential operator
M	mass per unit area or volume
M_n	effective mass of the n^{th} natural function q_n of a system
m	lumped mass
p, q	parameters that represent the mode shapes of a plate at resonance
q(x,y,z)	system displacement
$q_n(x,y,z)$	natural function of the n^{th} resonance of a system
$R_{g,a}$	Loss Factor Ratio: 20 $\log_{10}$ of the ratio of the measured loss factor of a particular resonance of a coated plate, air-loaded, to the measured loss factor of the corresponding resonance of the uncoated plate, air-loaded
$R_{g,w}$	Loss Factor Ratio: 20 $\log_{10}$ of the ratio of the measured loss factor of a particular resonance of a coated plate, water-loaded, to the measured loss factor of the corresponding resonance of the uncoated plate, water-loaded
$R_{g,w-a}$	Loss Factor Ratio: 20 $\log_{10}$ of the ratio of the measured loss factor of a particular resonance of the uncoated or a coated plate, water-loaded, to the measured loss factor of the corresponding resonance of the same plate, air-loaded
w	angular frequency of excitation
w_n	natural angular frequency of vibration
X(w)	Fourier transform of a system input
Y(w)	Fourier transform of a system output

y''	second derivative with respect to time of the displacement of a single-degree-of-freedom system
$\theta(w)$, $\theta(B)$	system phase

ACKNOWLEDGMENTS

The author wishes to express his sincere gratitude to Dr. John A. Macaluso and Dr. Geoffrey L. Wilson for their guidance and advice. Acknowledgments are also due Drs. Eugen J. Skudrzyk and Vernon H. Neubert for their helpful consultation.

This research was sponsored by the Applied Research Laboratory of The Pennsylvania State University under contract with the Naval Sea Systems Command.

CHAPTER I

INTRODUCTION

1.1 Background

Damping treatments that may be effective in reducing the vibration and sound radiation of fluid loaded plates are marketed commercially by numerous manufacturers. They are commonly available in two forms: as a semifluid, which must be applied with a spray gun or trowel; or as a prehardened sheet, which must be attached with an adhesive. Generally each manufacturer provides specifications of the decay rate, percent critical damping, effective temperature range, and material properties of their treatments. However, this information provides little insight into the effectiveness of these treatments in reducing the vibration and sound radiation of fluid-loaded plates.

Numerous investigations of the dynamic response and sound radiation of elastic structures in contact with a fluid have been made in the past. An excellent survey of prior work is given in the monograph by Firth (1977). Noteworthy contributions to the literature have come in recent years by Blake (1974), Davies (1971), Engblom and Nelson (1976), and Junger and Feit (1972). Leibowitz (1975) has written a comparative review of the analytical methods and results of several investigators, and provides a copious listing of references. Considered in these papers are the in-fluid response of elastic structures, such as beams, plates and shells, the effects of heavy fluid loading on this response,

and the radiation of energy into the fluid medium. Extensive theoretical analysis, and subsequent experimental work, has been done by these and other investigators. There is, however, very little published experimental data pertaining to the reduction of such vibrations and related sound radiation through the application of damping treatments. It is this general lack of such data that first provided the motivation and impetus for the experimental program described here.

1.2 Specific Statement of Problem

The aim of this investigation is twofold: (1) to measure the modal parameters and sound radiation of a center-driven, free, square plate (i.e., the reference plate) which is loaded either exclusively by a light fluid (air) on both sides, or on one side by a heavy fluid (water), and (2) to measure the modal parameters and sound radiation of center-driven, free, square plates which have damping treatments attached to one side, under similar fluid loading conditions. With these experiments, it has been possible to examine the effects of the heavy fluid loading and the damping treatments on the modal parameters of the plates. Also, the effects of the damping treatments on the sound radiation of the plates have been investigated. Since most structures can be decomposed into elements consisting of plates or shells, the results of these comparison tests are directly applicable to such structures.

1.3 Organization of Presentation

Chapter II investigates the vibrational characteristics of a center-driven, free, square plate under the two fluid loading conditions being considered. The theoretical resonant frequencies below 10 kHz of the air-loaded plate are determined, and the corresponding mode shapes are considered. Damping mechanisms which contribute to the dissipation of the vibrational energies of a plate are discussed. In the second part of Chapter II, the effects of heavy fluid loading are considered.

In Chapter III, consideration is given to the determination of the modal parameters using frequency response functions. The six mechanical response functions commonly used to determine these parameters are introduced, and in Section 3.2, the frequency response function of a damped, single-degree-of-freedom system is developed and discussed. In Section 3.3, the frequency response function of a uniform continuous system is considered. It is shown that, provided the criterion developed in Section 3.3 is satisfied, the modal parameters of mass, stiffness, and damping can be determined for each mode of a continuous system using the theory of systems with lumped-parameters, as developed in Section 3.2. In the last section of Chapter III, methods are developed which provide estimates of the mass, stiffness, and damping of a single-degree-of-freedom system.

In Chapter IV, the experimental apparatus, instrumentation and procedure are presented.

Chapter V contains the experimental results obtained for all plates. Measurements of the driving-point impedance of each plate, over

the frequency range of interest (0^+-10 kHz), are presented. The modal damping of each plate resonance within this region is determined for both fluid-loaded cases and compared with those of the reference plate. Frequency shift factors are introduced to describe the shift in the measured resonant frequencies caused by the various treatments and loading conditions. Changes in the loss factor of each resonance are expressed in terms of loss factor ratios. These ratios express in decibels (dB) the increase or decrease in the loss factor of each plate mode caused by the addition of the damping treatments and the change in the loading condition. In the second part of Chapter V, spectra of the sound levels measured in the test tank are presented and discussed. A direct comparison of the effects of the treatments on the noise radiated by the plates is possible.

Chapter VI summarizes the experimental results, and conclusions are drawn about the effects of the treatments on the vibrational characteristics and sound radiation of plates.

CHAPTER II

THE VIBRATION OF A CENTER-DRIVEN FREE SQUARE PLATE

2.1 Air-Loaded Case

A. Theoretical Resonant Frequencies and Mode Shapes. The tranverse vibrations of free, square plates has been considered by numerous authors. Waller (1939) briefly outlined the historical background, and described the results of a systematic study she conducted on the normal vibrations of free, square plates. Warburton (1954) applied the Rayleigh method, assuming waveforms similar to those of a beam, to derive approximate frequency expressions for the transverse modes of vibration of rectangular plates.

For a free plate which is square or almost square, both Waller and Warburton noted the existence of degenerate modes where the nodal patterns do not consist of lines parallel to the sides of the plate. Also they found that a square plate does not have two normal modes, p/q, q/p, with identical frequencies, but rather, has normal modes represented by $p/q \pm q/p$ with two discrete frequencies. Here the parameters p and q represent the modes of the plate at resonance. For the center-driven, free, square plate, only the p/q modes are excited, where p and q are even and $p-q = 0,2,4,6,\ldots$ When p=q, the patterns have nodal lines which are parallel to the sides of the plate. For the case where $p-q = 2,4,6,\ldots$, the modes excited are of the degenerate type, denoted by p/q+.

Selected Chladni's drawings of the normal mode system of a free, square plate, which were presented by Waller (1939), are seen in Figure 1. For the center-driven plate being considered in this investigation, it has been found that the modes excited are the 2/0+, 2/2, 4/0+, 4/2+, 4/4, 6/0+,... type (Section 5.1).

The experiments to be described always utilized center-driven, aluminum plates that were 12.0 in. square, 0.375 in. thick, and unconstrained along all edges. The theoretical resonant frequencies of these plates, calculated from expressions derived by Warburton, appear in the second column of Table I.

B. Damping Mechanisms. There are several damping mechanisms which can contribute to the dissipation of the vibrational energies of a plate. They are commonly grouped into two classifications; (1) material damping, or mechanical hysteresis, and (2) system damping, which includes acoustic radiation, damping due to applied treatments, and interface friction. The three which have been of major concern with respect to this investigation are material damping, radiation damping, and damping due to applied treatments.

1. Material Damping. The energy dissipation properties of a linear, viscoelastic material subjected to time dependent variations of stress and strain are commonly represented by the complex modulus

$$k^* = k(1+ jg_m) \quad , \qquad [2.1]$$

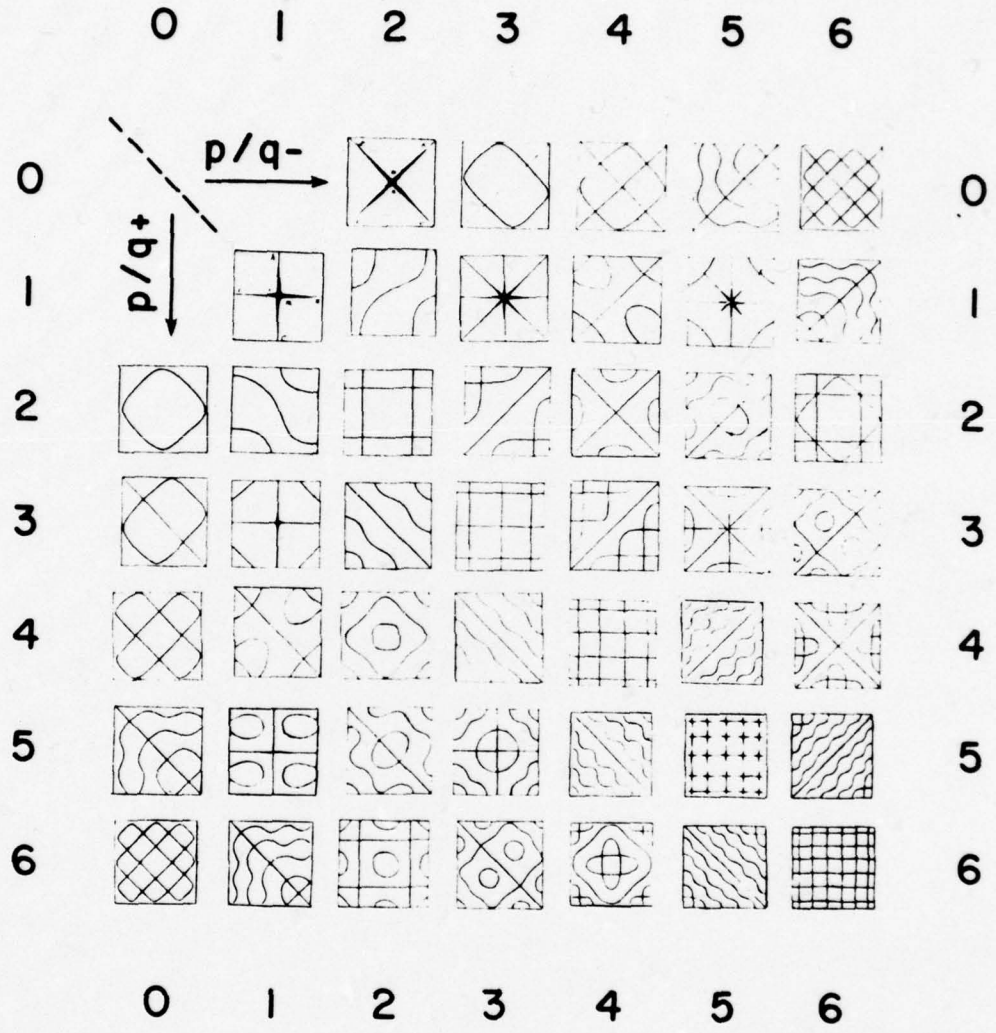

Figure 1. Selected Chladni's drawings, presented by Waller (1939), of the normal mode system of a free, square plate.

TABLE I

THEORETICAL RESONANT FREQUENCIES FOR A CENTER-DRIVEN FREE SQUARE (12.0 x 12.0 x 0.375 in.) ALUMINUM PLATE

p/q	Theoretical Resonant Frequencies (Hz)
2/0+	623.2
2/2	1670.9
4/0+	3115.7
4/2+	4331.0
4/4	7243.9
6/0+	7597.5
6/2+	8825.5

where g_m is the material loss factor, and k is the stiffness constant. All materials exhibit this property of mechanical hysteresis under oscillatory strain. The extent to which they dissipate energy internally by this damping mechanism is dependent on the loss factor of the material. Most structural metals, such as aluminum and steel, have very low internal damping; their loss factors are typically on the order of 10^{-5} to 10^{-4}.

2. Damping by Applied Treatments. A common method of increasing the loss factor of a structure consists of the attachment of one or more layers of a viscoelastic material with a high material loss factor to its major surface areas. The resulting composite material will have a greater capability to dissipate energy internally than the original one.

In considering the use of damping treatments in order to increase the energy dissipation capabilities of a plate, it is noted that there are two basic system configurations which are commonly used. The simplest system consists of the attachment of an unconstrained layer of treatment to the surface of the plate. Because the material loss factor of the plate is typically very low, it can be assumed that all energy dissipation occurs due to extensional strain of the damping layer during flexure of the plate, and the loss factor of the composite plate may be considered to be that of the treatment. The second configuration is that of a constrained damping layer, where a layer of treatment is sandwiched between two plates. This configuration was not considered in

this investigation.

3. Radiation Damping. The dissipation of the vibrational energies of a plate may be due in part to the transfer of energy to the surrounding medium in the form of acoustic waves. These radiation characteristics may be described in terms of the radiation loss factor g_r, which indicates the extent to which the vibration of a system is damped due to the radiation of energy from the structure to the ambient medium. For the case of an air-loaded plate, the acoustic-structure interaction is weak and the radiation loss factor can be considered negligible; however, this assumption is not possible when considering water loading.

2.2 Water-Loaded Case

The dynamic characteristics of a vibrating plate in contact with water are changed by the water loading and radiation damping. Because the specific acoustic impedance of structural metals, such as aluminum and steel, is similar to that of water, there exists a strong acoustic-structure interaction resulting in fluid-structure coupling.

The results of this strong coupling are (1) an increased radiation loss factor, (2) the addition of an inertia term which results in an increase in the dynamic mass of the plate, and (3) a cross coupling of the vibrational modes of the plate.

CHAPTER III

DETERMINATION OF MODAL PARAMETERS

3.1 Frequency Response Functions

The dynamic characteristics of a constant-parameter linear system can be described by its frequency response function H(w), which is defined as:

$$H(w) = \frac{Y(w)}{X(w)} \quad , \qquad [3.1]$$

where X(w) is the Fourier transform of the system input, and Y(w) is the Fourier transform of the system output. A physically realizable, stable system will have a unique frequency response function which will be a function of frequency only, and not a function of either time or the applied input.

In general, the frequency response function is a complex valued quantity, which may be expressed in complex polar notation as:

$$H(w) = |H(w)|e^{-j\theta(w)} \quad . \qquad [3.1a]$$

The absolute value |H(w)| is called the magnitude or gain factor of the system, and $\theta(w)$ is known as the system phase. Alternatively, H(w) may be written:

$$H(w) = H_R(w) + jH_I(w) \quad , \qquad [3.1b]$$

where the real part $H_R(w)$ and imaginary part $H_I(w)$ are commonly referred to as the coincident and quadrature components of H(w), respectively.

The frequency response functions commonly used in determining the dynamic characteristics of structures are:

1) Dynamic Compliance (displacement/force)

2) Mobility (velocity/force)

3) Accelerance (acceleration/force)

4) Dynamic Stiffness (force/displacement)

5) Impedance (force/velocity)

6) Effective Mass (force/acceleration)

The dynamic compliance, mobility, and accelerance functions are all complex ratios of an output response to input force, as defined by Equation [3.1]. The magnitudes of these functions all reach maxima at resonance. The impedance, dynamic stiffness, and effective mass are defined by the complex ratio of the force input to system response and, as such, are the reciprocals of the dynamic compliance, mobility, and accelerance, respectively. These functions reach miminum values at resonance. When the input force and output response are measured at the same point and in the same direction, the ratio is designated a driving-point ratio (i.e., driving-point impedance, driving-point mobility, etc.).

The dynamic information contained in these mechanical response functions is the same and, therefore, having knowledge of one is

equivalent to having knowledge of all six.

3.2 The Frequency Response Function of a Damped Single-Degree-of-Freedom System

The equation of motion of a sinusoidally excited, hysteretically damped, single-degree-of-freedom system is:

$$my'' + k(1+jg)y = Xe^{jwt} \quad , \qquad [3.2]$$

where Xe^{jwt} is the complex form of the applied force, m and k the system mass and stiffness, respectively, g the loss factor, w the frequency of excitation, and y the system displacement. Hysteretic damping is introduced into this equation as the complex elastic modulus $k^* = k(1+jg)$. The steady state solution can be represented by:

$$y = Ye^{jwt} \quad . \qquad [3.3]$$

Substituting into Equation [3.2], we have:

$$\{-mw^2 + k(1+jg)\}\, Y = X \qquad [3.4]$$

or

$$\frac{Y}{X} = \frac{1}{\{k - mw^2 + jkg\}} \quad . \qquad [3.5]$$

Introducing the parameter $B = \frac{w}{w_n}$, where $w_n^2 = \frac{k}{m}$ is the natural frequency of undamped vibration, the previous equation can be written:

$$\frac{Y}{X} = \frac{1}{k\{1 - B^2 + jg\}} \quad , \qquad [3.6]$$

which is equivalent to the frequency response function H(B) of a hysteretically damped, single-degree-of-freedom system. Therefore,

$$H(B) = \frac{1}{k\{1 - B^2 + jg\}} \quad . \qquad [3.7]$$

Noting that H(B) is a complex valued quantity, it can be written in polar notation as:

$$H(B) = |H(B)|e^{-j\Theta(B)} \quad , \qquad [3.8]$$

where

$$|H(B)| = \frac{1/k}{\sqrt{(1 - B^2)^2 + g^2}} \qquad [3.8a]$$

and

$$\Theta(B) = \tan^{-1}\left(\frac{g}{1 - B^2}\right) \quad . \qquad [3.8b]$$

The magnitude $|H(B)|$ has units of $(\text{stiffness})^{-1}$ or displacement/force and is therefore equivalent to the mechanical compliance of the system.

In terms of real (coincident) and imaginary (quadrature) components, the frequency response function expressed in Equation [3.7] can be written:

$$H(B) = H_R(B) - jH_I(B) \quad , \qquad [3.9a]$$

where

$$H_R(B) = \frac{(1-B^2)\ (1/k)}{(1-B^2)^2 + g^2} \qquad [3.9b]$$

and

$$H_I(B) = \frac{g\ (1/k)}{(1-B^2)^2 + g^2} \quad . \qquad [3.9c]$$

Figures 2 and 3 give plots of $|H(B)|$, $\Theta(B)$, $|H_R(B)|$, and $H_I(B)$ versus B for a loss factor g = 0.1 and stiffness constant k = 1.0. Note that, at resonance (i.e., when B = 1.0), the magnitude $|H(B)|$ and quadrature $H_I(B)$ reach maxima of equal response, and the phase $\Theta(B)$ and coincidence $|H_R(B)|$ pass through points of maximum inflection. Also, $\Theta(B)$= 90 degrees and $|H_R(B)| = 0$ at resonance.

3.3 The Frequency Response Function of a Uniform Continuous System

The differential equation of motion of a periodically forced, uniform, continuous system, such as the plate being considered here, can be written in the form:

$$-Mw^2 q(x,y,z) + K^* Lq(x,y,z) = f(x,y,z) \quad , \qquad [3.9]$$

where $f(x,y,z)$ is the external harmonic force exerted on the system per unit area or volume, $q(x,y,z)$ is the system displacement, which can be

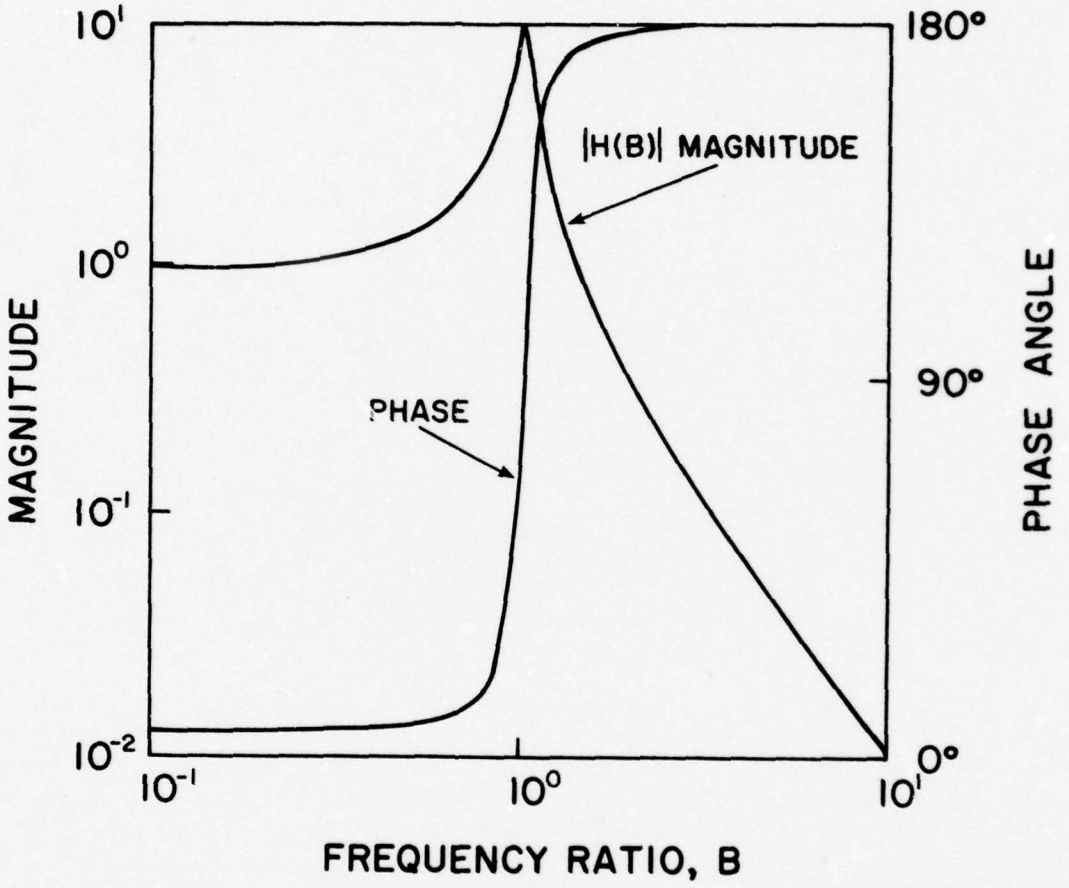

Figure 2. Magnitude and phase of a single-degree-of-freedom system with a loss factor g= 0.1 and stiffness constant k= 1.0. The system resonance occurs at B= 1.0, where $B=\frac{w}{w_n}$.

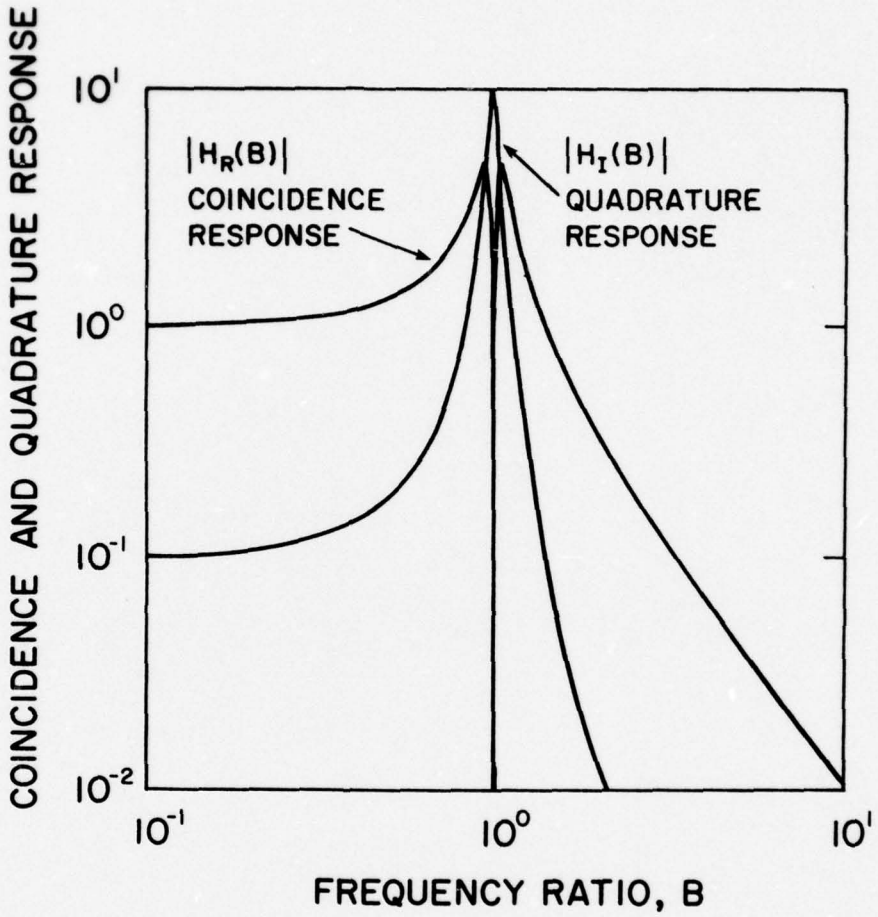

Figure 3. Real (coincidence) and imaginary (quadrature) components of a single-degree-of-freedom system with a loss factor g= 0.1 and stiffness constant k= 1.0. The system resonance occurs at B=1.0, where $B=\frac{w}{w_n}$.

resolved into a summation of natural functions $q_n(x,y,z)$, K^* is the complex elastic modulus used to account for hysteretic damping, and L is the linear differential operator working on $q(x,y,z)$ to give the effective strain in the system. Skudrzyk (1958) has reduced this relationship to the form,

$$\{-M_n w^2 + K_n(1+ jG_n)\}\, q_n = f_o \quad , \qquad [3.10]$$

where M_n, K_n, and G_n represent the effective mass, stiffness, and loss factor for the n^{th} natural function q_n of the system. In form, this equation is identical to the response equation of a single-degree-of-freedom system, as expressed in Equation [3.4]. Thus, the response of any normal mode of a uniform, continous system can be treated as that of a single-degree-of-freedom system with parameters M_n, K_n, and G_n. The total response of the system is given by the summation of the modal responses:

$$q(x,y,z) = \sum q_n(x,y,z) = f_o \sum \frac{1}{\{-M_n w^2 + K_n(1+ jG_n)\}} \quad . \qquad [3.11]$$

This equation states that the excitation of a continuous system at one of its natural frequencies w_n will result in a response which is a summation of the response of the resonating mode and an infinite summation of nonresonating modes. The contributions of the nonresonating modes to the total response at w_n is dependent on their resonant frequencies and damping. For low-order modes which are

sufficiently isolated from other natural frequencies, the concepts developed for a single-degree-of-freedom system are applicable in evaluating the modal parameters.

The response of a continuous system being driven at a given forcing frequency w will be dominated by the response of one resonating mode without substantial contribution by others if:

$$dw >> w_n g_n \quad , \qquad [3.12]$$

where $w_n g_n$ is the mode bandwidth at the usual half-power points, assuming low damping ($g^2 << 1$), and dw is the frequency spacing between successive modes. Thus, complete determination of modal parameters using the theory of systems with lumped-parameters is possible provided the criterion expressed in Equation [3.12] is followed.

3.4 Mass and Stiffness

A means of estimating the modal mass and stiffness of a mechanical system is provided by a log-log plot of its frequency response function. Consider, for example, the magnitude of the compliance of a simple, mass-spring system:

$$|H(w)| = \frac{1}{k - w^2 m} \quad . \qquad [3.13]$$

At low frequencies, $k >> w^2 m$ and the magnitude $|H(w)|$ is stiffness controlled, such that the function is constant with frequency. At high

frequencies, $k << w^2m$, and the magnitude is mass controlled, such that $|H(w)|$ decreases essentially in proportion to frequency squared. When the function presented in Equation [3.13] is displayed in a log-log plot, these regions of stiffness and mass control approach asymptotic slopes of 0 and -2 (-12dB/octave), respectively. Thus, the asymptotic slope values in a log-log presentation of any of the six mechanical response functions (Section 3.1) can be used to estimate the effective mass and stiffness of a mechanical system.

3.5 Damping

Damping is assumed to be of the form expressed in Equation [2.1]. The loss factor can be determined using any one of the following methods, each of which assumes a single-degree-of-freedom response:

1) From the magnitude of the frequency response function, it can be shown that:

$$\varepsilon = \frac{w_1 - w_2}{w_n} \quad , \qquad [3.14]$$

where w_1 and w_2 are the frequencies on each side of w_n where the response is 3 dB down from the response at resonance.

2) The loss factor can be determined from the coincident component of the frequency response, which is written in the nondimensional form:

$$H_R(B)k = \frac{1 - B^2}{(1 - B^2)^2 + g^2} \quad . \qquad [3.15]$$

By differentiating, the frequencies of maximum response can be determined as:

$$w_1 = w_n \sqrt{1+ g}$$

and

$$w_2 = w_n \sqrt{1- g} \quad ,$$

or

$$w_1^2 = w_n^2 \ (1+ g)$$

and

$$w_2^2 = w_n^2 \ (1- g) \quad .$$

Solving for w_n^2 and equating:

$$\frac{w_1^2}{1+ g} = \frac{w_2^2}{1- g} \quad .$$

Solving for the loss factor g, the relationship

$$g = \frac{(w_1/w_2)^2 - 1}{(w_1/w_2)^2 + 1} \qquad [3.16]$$

is derived. Using this equation, the damping factor can be determined from the knowledge of the coincident component of the frequency response.

3) Using the quadrature component of the frequency response, which is written in the nondimensional form:

$$H_I(B)k = \frac{g}{(1- B^2)^2 + g^2} \quad , \qquad [3.17]$$

the loss factor g can be calculated. At resonance,

$$H_{Imax}k = \frac{1}{g} \quad , \qquad [3.18]$$

which is the maximum response of the system. Now, at frequencies w_1 and w_2 on each side of w_n where the amplitude is one-half the response at resonance, Equation [3.17] can be written:

$$H_I k = \frac{g}{\left[1-\left(\frac{w_n - \frac{dw}{2}}{w_n}\right)^2\right]^2 + g^2} \quad , \qquad [3.19]$$

where $\frac{dw}{2} = \frac{w_1 - w_2}{2}$. By neglecting the $\left(\frac{dw}{2w_n}\right)^2$ term, Equation [3.19] can be written:

$$H_I k \approx \frac{g}{\left(\frac{dw}{w_n}\right)^2 + g^2} \quad . \qquad [3.20]$$

Therefore, from Equations [3.18] and [3.20], the following ratio can be written:

$$\frac{H_{Imax}}{H_I} = \frac{\left(\frac{dw}{w_n}\right)^2 + g^2}{g^2} \quad . \qquad [3.21]$$

Solving this equation for g, the loss factor, and noting that $\frac{H_{Imax}}{H_I} = 2$, it can be shown that:

$$g = \frac{w_1 - w_2}{w_n} \quad , \qquad [3.22]$$

which indicates the use of the quadrature component of the frequency response function in determining the damping.

These three methods are equivalent for a lightly damped single-degree-of-freedom system. For a continous system, where the criterion expressed in Equation [3.12] is followed, methods 2 and 3 are commonly used.

CHAPTER IV

EXPERIMENTAL APPARATUS AND PROCEDURE

4.1 Plate Specimens

The specimens used in this investigation consisted of five 12.0 in. x 12.0 in. x 0.375 in. aluminum plates, pictured in Figure 4. Threaded into holes at the center of each were 3/8-16 UNC threaded studs. These protruded 5/16 in. outward from the upper surface and were used to attach the plates to the driver.

4.2 Damping Treatments

The damping treatments tested included GP-1, Epoxy 10 and Embossed Foam Damping Sheet (VE), all products of the Soundcoat Corporation, and LD400, a product of the Lord Corporation. GP-1 and Epoxy 10 were supplied as semifluids. These were troweled onto the upper surface of the plates to a thickness of approximately 0.25 in. in accordance with manufacturer's specifications. LD400 and VE were supplied as prehardened sheets 0.25 in. thick. These were attached to the upper surface of the plates with epoxy compounds as recommended by the manufacturers. The VE treatment was originally supplied with an upper layer of acoustic foam. This foam was intended for use in attenuating airborne sound incident upon it and does not contribute to the vibration damping characteristics of the treatment. It was removed prior to testing of the VE coated plate.

REFERENCE PLATE

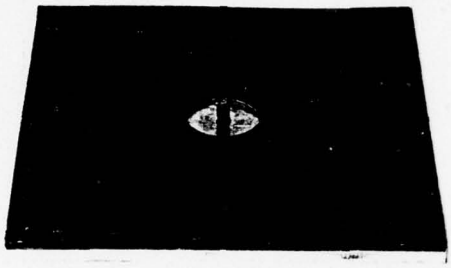

LD 400

GP-I

EMBOSSED FOAM
DAMPING SHEET (VE)

EPOXY 10

Figure 4. Photograph of aluminum plate specimens.

A circular section of treatment, 2.25 in. in diameter, was removed from each coated plate (see Figure 4). This was necessary in order to accommodate the shape of the bottom of the driver.

One plate was left uncoated. This was used as reference, to which all coated plates were compared. Throughout this report, this uncoated plate is referred to as the reference plate.

4.3 Suspension Apparatus

A diagram of the experimental apparatus used to suspend and drive the plates is seen in Figure 5. This apparatus consisted of a Wilcoxon Model F4 electromagnetic driver with Z820 impedance head. Secured around the outer casing of the driver was a worm gear type hose clamp to which four mounting brackets were welded. The driver was suspended by this hose clamp from two elastic shock cords. The plates were attached to the driver by their threaded studs. Under this drive configuration, the plates were unconstrained along all edges. The resonant frequency of the driver-plate system suspended by the elastic cords was determined to be far below the first resonance of any of the plates.

The water-loaded phase of investigation was conducted at the test tank facility of the Applied Research Laboratory at The Pennsylvania State University. This tank is 26 ft. x 17.5 ft. x 18 ft. deep. Using a telescoping array holder, the entire suspension apparatus was lowered into this tank until the bottom side of the plate being tested made contact with the water. Lowering was continued until the water reached the top edge of the plate, as shown in Figure 5. The position of the

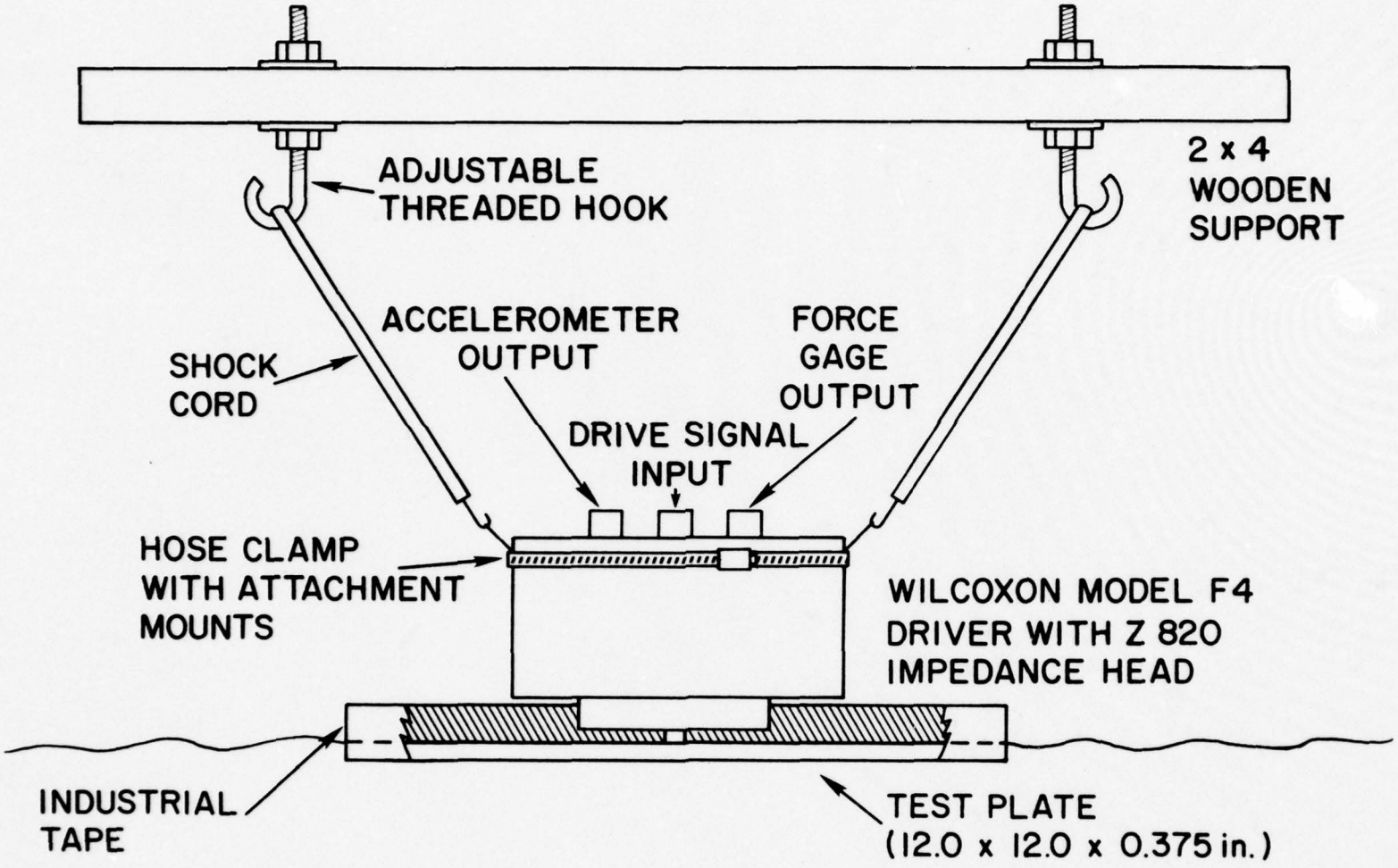

Figure 5. Experimental apparatus.

plates relative to the tank walls was found to have no detectable effect on their vibrational characteristics; however, in their normal test position, the plates were situated such that the distance to the nearest wall was maximized. Industrial tape was attached around all edges of the plates to assure that water did not flow onto their upper sides or against the damping treatments. Comparison of the driving-point impedance of the air-loaded reference plate, with and without the tape attached, showed that the tape had no detectable effects on the modal characteristics of the plate.

4.4 Instrumentation

A block diagram of the electronic system is shown in Figure 6. Basically, an automatic sweep sinewave generator, or a random noise generator, produced a signal which was amplified and fed to the driver, which excited the test plate centrally. A force gage and accelerometer mounted internally in the impedance head sensed the input force to the plate and resultant motions at the drive point. After preamplification of their signals, that portion of the measured force signal introduced by the mass between the bottom of the force gage and the plate was cancelled electronically by the mass cancellation system, as discussed in Appendix A. The accelerometer and corrected force signals were then fed into a two-channel digital signal processor for analysis.

The two-channel processor used during the majority of the experimental period was a Spectral Dynamics Model SD360. The force and accelerometer signals fed into this processor were used to develop any

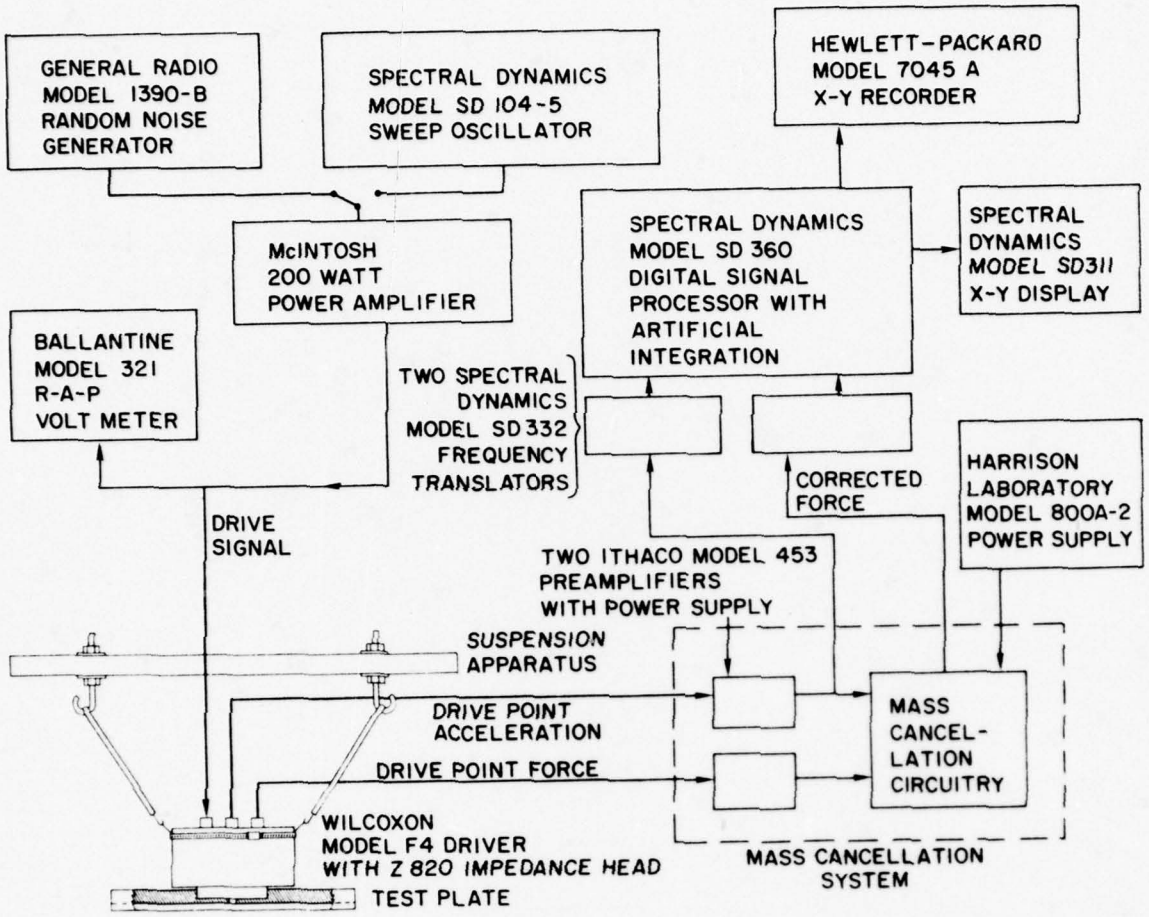

Figure 6. Block diagram of the electronic system used in the measurement of the mechanical impedance of the plates.

one of the six mechanical response functions. Peripherals associated with this processor included two Spectral Dynamics Model SD332 Frequency Translators, a Spectral Dynamics Model SD311 X-Y Display, and a Hewlett-Packard Model 7045A X-Y Recorder. The frequency translators enabled accurate measure of the resonant frequencies and loss factors of each plate mode by effectively "zooming" in on selectable frequency bands and increasing the frequency resolution of the processor. The X-Y display and recorder provided a visual display of the measured response function and recording capabilities.

4.5 System Calibration

System calibration was done in accordance with standard industrial techniques. This involved loading the driver with a known weight which was then excited either sinusoidally or with broad band random noise, over the frequency range of interest. At frequencies above the first resonance of the driver (approximately 30 Hz for the Wilcoxon F4 driver used), the mechanical response function measured will approach an asymptotic value equal to the effective mass of the weight being driven plus the mass below the force gage. Thus, a means of system calibration is provided. A typical calibration spectrum is seen in Figure 7, which is the measured driving-point impedance of a 4.37 lb. mass.

4.6 Determination of Mode Shapes

The mode shapes of the first six resonances of the reference plate were measured in order to determine the order of the modes of vibration.

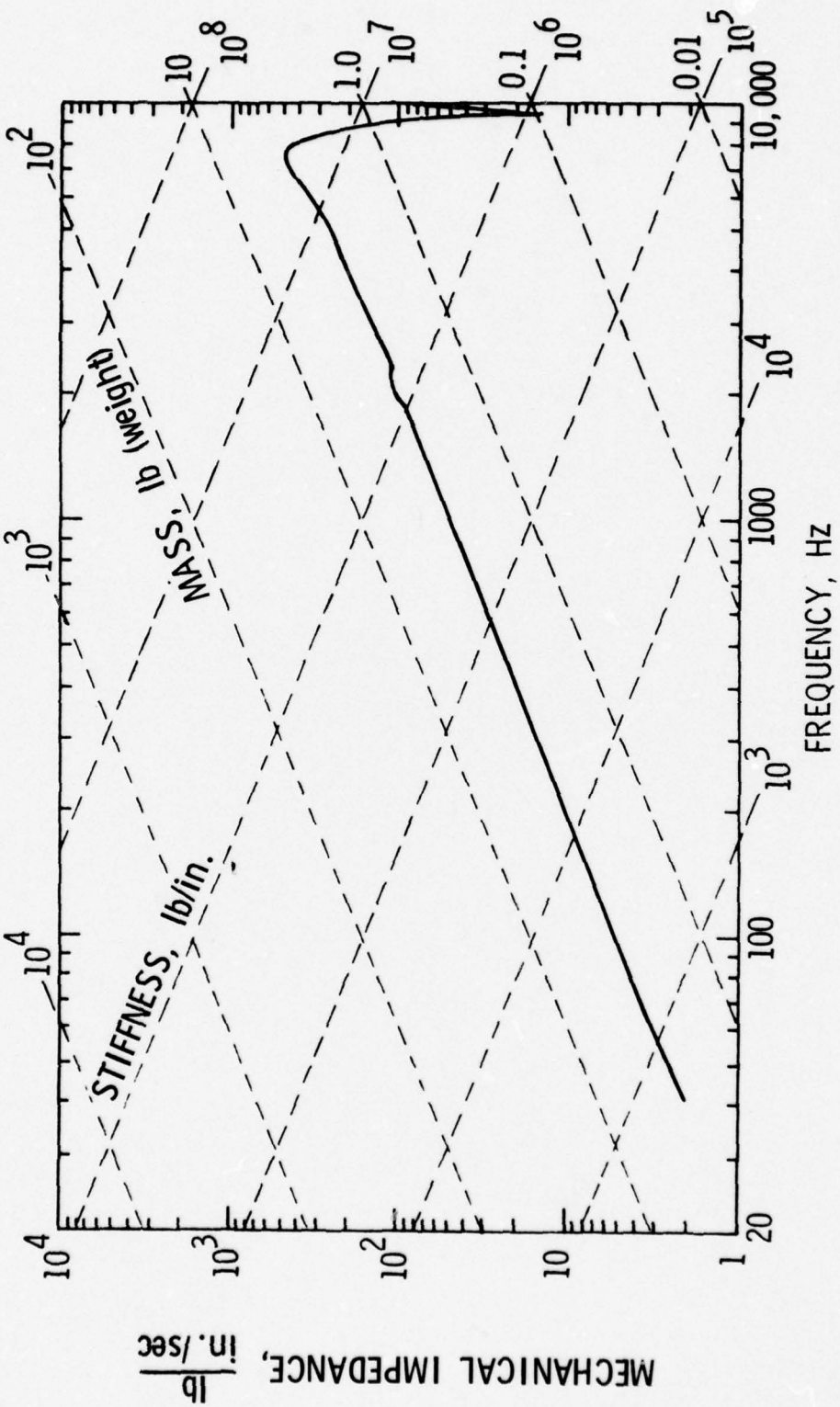

Figure 7. Measured driving-point impedance of a 4.37 lb. mass used during system calibration.

This was done by exciting the plate centrally at each resonant frequency and measuring the acceleration at selected locations on the surface of the plate. A BBN accelerometer with double-sided adhesive tape was used to measure the acceleration. The mode shapes were determined by first normalizing the measured acceleration levels and then noting the locations of nodal lines. A square grid, scribed on the surface of the plate, was used to determine the measurement locations.

4.7 Radiation Measurements

Noise radiated into the test tank by the water-loaded plates was measured using an Aquadyne Type H23 hydrophone. This hydrophone was positioned horizontally 6 ft. below the water-loaded test plate. In this position, the hydrophone was in the direct sound field of the plate. The shaker was driven with wide band random noise (0^{+}-10 kHz), and the spectrum of the sound level measured in the test tank was developed by the Spectral Dynamics Model SD360 Digital Signal Processor.

CHAPTER V

DISCUSSION OF RESULTS

5.1 Air-Loaded Case

A. Reference Plate. The measured driving-point impedance of the reference plate is plotted in Figure 8. In this figure, resonances appear as minima in the function, and antiresonances appear as peaks. Asymptotic lines of +1 and -1 slope have been drawn to aid in identifing mass and stiffness terms (Section 3.4). Dynamic range limitations of the SD360 Signal Processor have resulted in clipping of several of the lower order antiresonant peaks, resulting in the appearance of a curious double notching. Wherever this occurred, the region was examined in more detail using the zoom feature provided by the SD332 Frequency Translators, and the corrected values were measured. These have been drawn in as dashed lines on the original plots. Listed in Table II are the theoretical resonant frequencies (Section 2.1), measured resonant frequencies, percentage deviation between these frequencies, and relevant mode designations p/q. Note that all measured resonant frequencies listed fall within 6 percent of their theoretical values. The mode shapes of the first six resonances were measured using the method described in Section 4.6. These agreed with the mode shapes observed by Waller (Section 2.1), identifying the modal parameters p and q for each resonance.

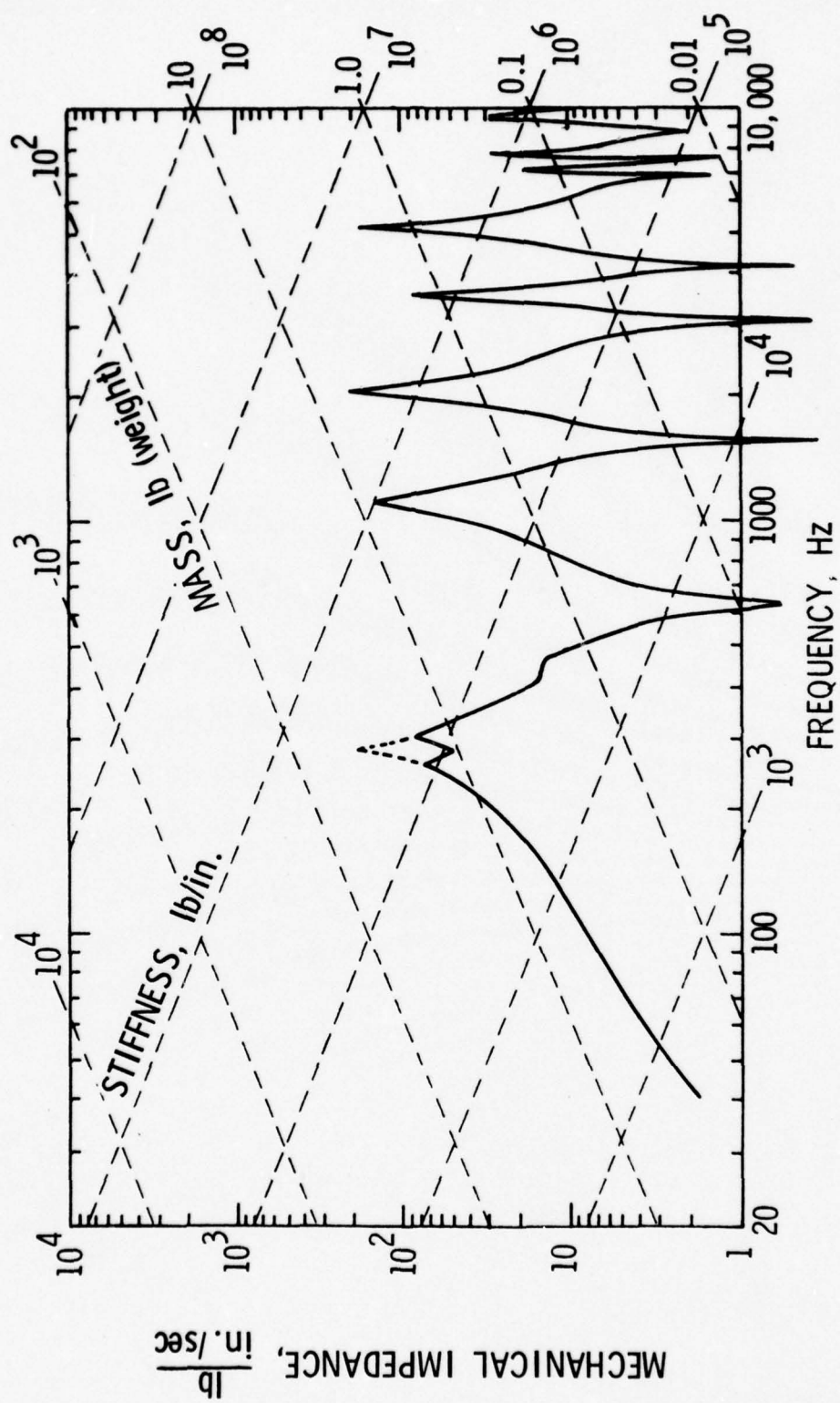

Figure 8. Measured driving-point impedance at the center of the square (12.0 x 12.0 x 0.375 in.) aluminum reference plate.

TABLE II

THEORETICAL AND EXPERIMENTAL RESONANT FREQUENCIES AND PERCENTAGE DEVIATION FOR THE CENTER-DRIVEN FREE SQUARE (12.0 x 12.0 x 0.375 in.) ALUMINUM PLATE

p\q	Theoretical Resonant Frequencies (Hz)	Experimental Resonant Frequencies (Hz)	Percentage Deviation
2/0+	623.2	637.8	2.25
2/2	1670.9	1605.8	3.95
4/0+	3115.7	3133.8	0.58
4/2+	4331.0	4205.4	2.79
4/4	7243.9	6822.5	5.83
6/0+	7597.5	7442.5	2.05
6/2+	8825.5	8840.0	0.17

B. Coated Plates. Analysis of the measurements of the coated plates is facilitated by the introduction of a Frequency Shift Factor and a Loss Factor Ratio. A Frequency Shift Factor, denoted $D_{f,a}$, is defined as the ratio of the measured resonant frequency of a coated plate, air-loaded, to the corresponding measured resonant frequency of the reference plate, air-loaded. A Shift Factor greater or less than unity indicates that a resonance has moved to a higher or lower frequency by the attachment of the damping treatment. A change in the loss factor caused by the treatments is expressed in terms of a Loss Factor Ratio $R_{g,a}$, which is defined in decibels as 20 $\log_{10}$ of the ratio of the measured loss factor of a particular resonance of a coated plate, air-loaded, to the measured loss factor of the corresponding resonance of the reference plate, air-loaded. An increase or decrease in the loss factor is then reflected as a positive or negative value of $R_{g,a}$ in decibels (dB).

The measured driving-point impedance of the LD400 coated plate is plotted in Figure 9. Addition of this damping tile is seen to suppress the resonant "valleys" throughout the frequency range considered. The increase in the loss factor of each resonance, as reflected by the Loss Factor Ratio $R_{g,a}$, and the change in the resonant frequencies, as expressed in terms of the Frequency Shift Factor $D_{f,a}$ are given in Table III. Note that the Frequency Shift Factors $D_{f,a}$ are greater than unity for all modes, indicating a general shift upward in frequency. This can be attributed to an overall increase in the stiffness of each plate mode due to the attachment of the treatment. Asterisks(*) in this table, and

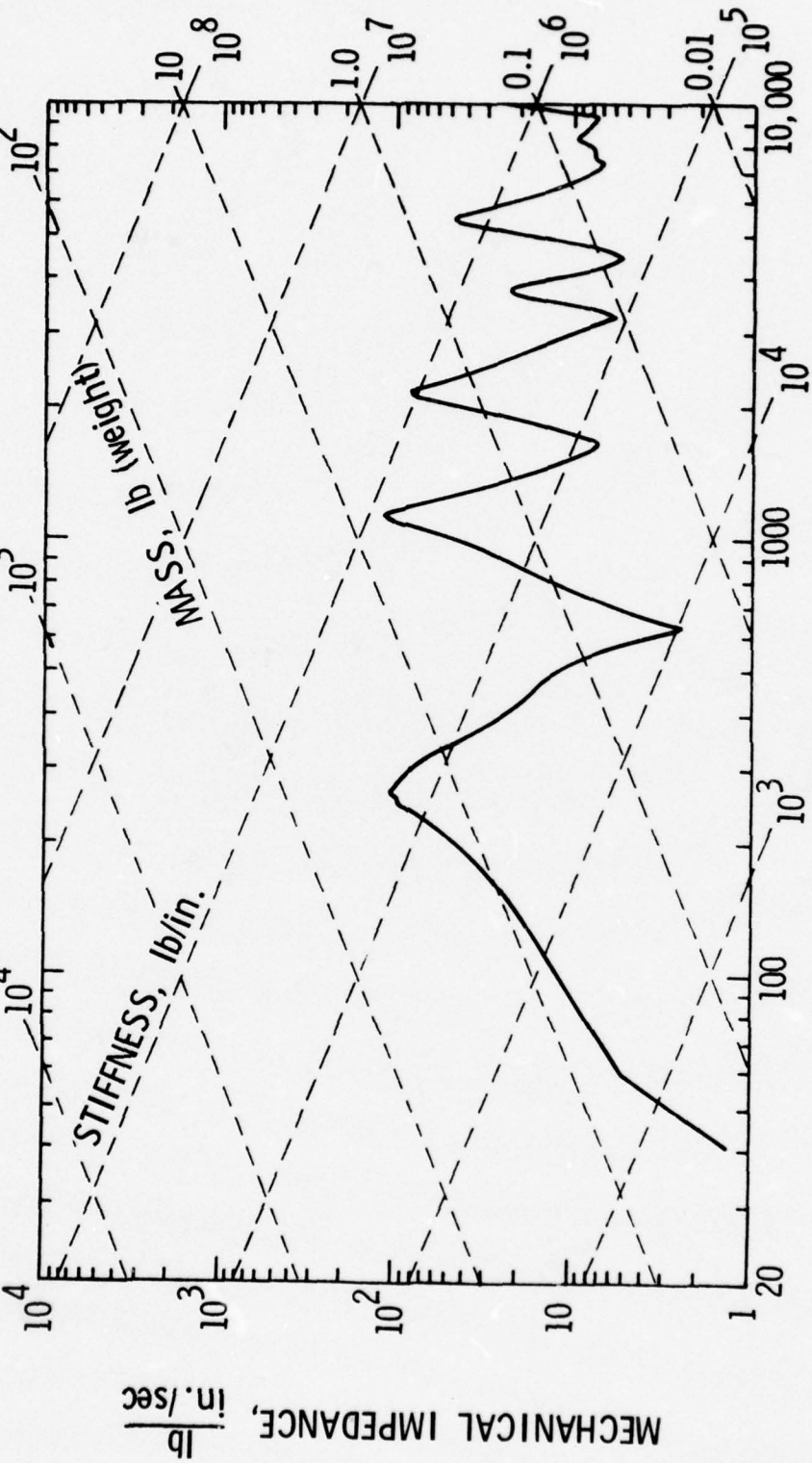

Figure 9. Measured driving-point impedance at the center of a uniform aluminum plate (12.0 x 12.0 x 0.375 in.) coated with a 0.25 in. thick layer of LD400 damping treatment.

TABLE III

FREQUENCY SHIFT FACTOR $D_{f,a}$ AND LOSS FACTOR RATIO $R_{g,a}$ FOR THE AIR-LOADED SQUARE PLATE COATED WITH LD400 DAMPING TILE

p/q	Frequency Shift Factor $D_{f,a}$	Loss Factor Ratio $R_{g,a}$ (dB)
2/0+	1.01	50.5
2/2	1.05	37.7
4/0+	1.05	29.2
4/2+	1.05	29.1
4/4	1.06	*
6/0+	1.04	*
6/2+	1.02	*

all subsequent tables, indicate that the criterion expressed in Equation [3.12] was not satisfied by the corresponding resonance. As a result, the loss factor of that mode could not be accurately determined using the methods outlined in Section 3.5.

Similar data was measured for the GP-1, VE, and Epoxy 10 coated plates, and is illustrated in Figures 10 through 12. Values of the Loss Factor Ratio $R_{g,a}$ and Frequency Shift Ratio $D_{f,a}$ for these three cases are tabulated in Tables IV through VI. Note that both the GP-1 compound and the VE damping tile have caused an upward shift of the resonant frequencies, indicated by the Frequency Shift Ratios, which are greater than unity. Note also that a downward shift of the resonant frequencies has been caused by the Epoxy 10 compound. Of the four compounds tested, LD400 and VE are seen to have the greatest Loss Factor Ratios.

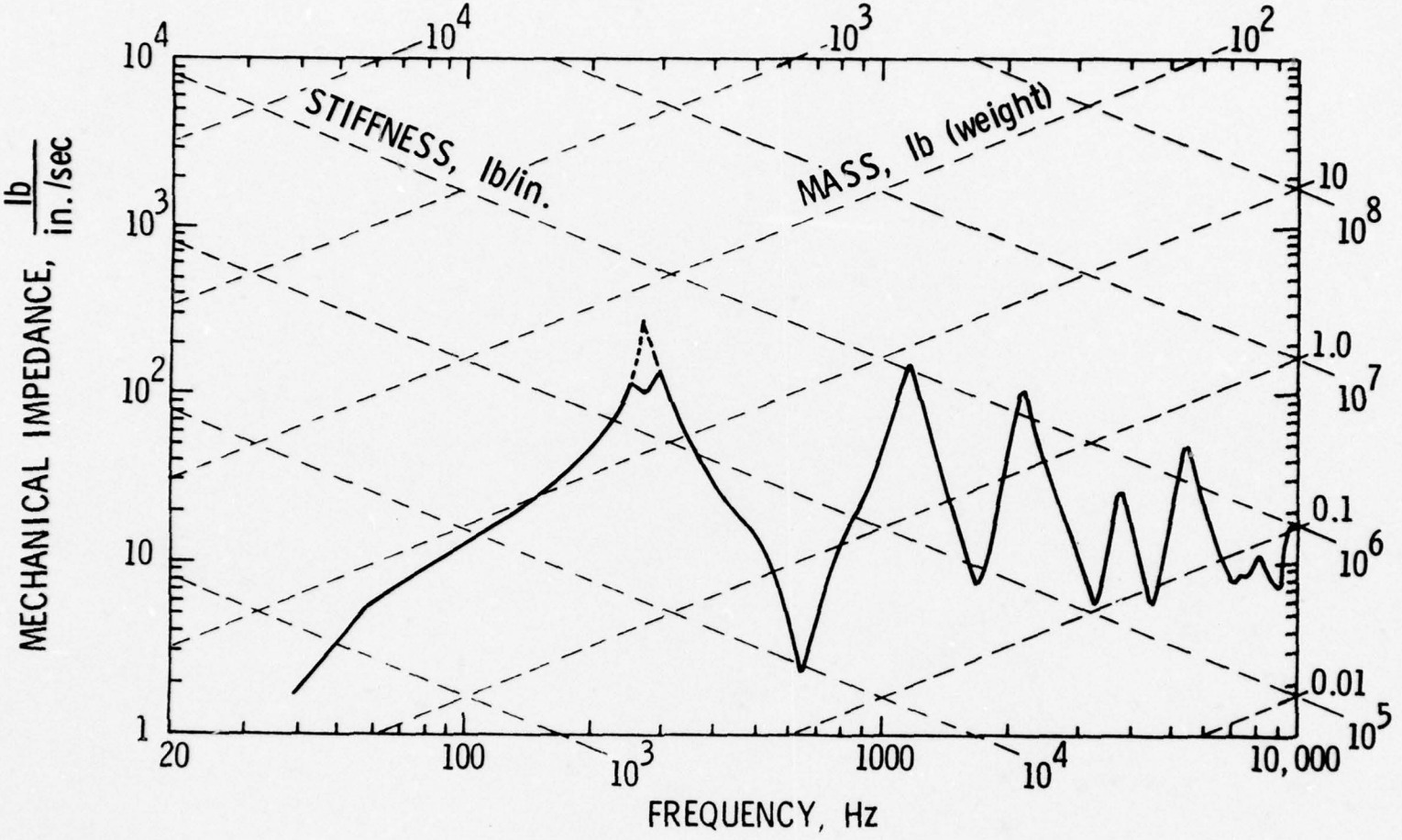

Figure 10. Measured driving-point impedance at the center of a uniform aluminum plate (12.0 x 12.0 x 0.375 in.) coated with a 0.25 in. thick layer of GP-1 damping treatment.

TABLE IV

FREQUENCY SHIFT FACTOR $D_{f,a}$ AND LOSS FACTOR RATIO $R_{g,a}$ FOR THE AIR-LOADED SQUARE PLATE COATED WITH GP-1 DAMPING COMPOUND

p/q	Frequency Shift Factor $D_{f,a}$	Loss Factor Ratio $R_{g,a}$ (dB)
2/0+	1.17	44.3
2/2	1.24	29.8
4/0+	1.18	22.5
4/2+	1.18	21.7
4/4	1.13	34.6
6/0+	1.11	41.6
6/2+	1.10	*

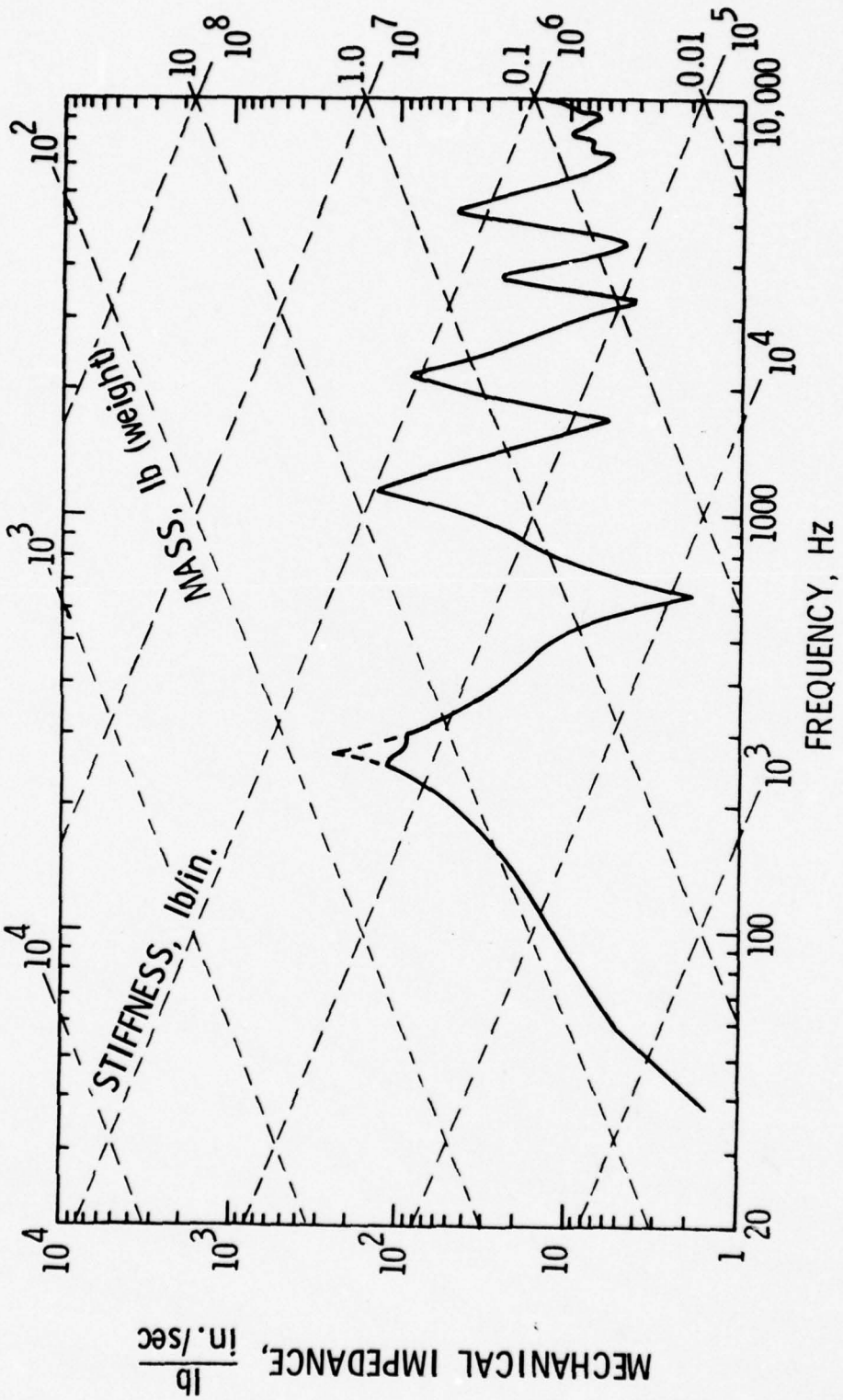

Figure 11. Measured driving-point impedance at the center of a uniform aluminum plate (12.0 x 12.0 x 0.375 in.) coated with a 0.25 in. thick layer of Embossed Foam Damping Sheet (VE).

TABLE V

FREQUENCY SHIFT FACTOR $D_{f,a}$ AND LOSS FACTOR RATIO $R_{g,a}$ FOR THE AIR-LOADED SQUARE PLATE COATED WITH VE DAMPING TILE

p/q	Frequency Shift Factor $D_{f,a}$	Loss Factor Ratio $R_{g,a}$ (dB)
2/0+	1.07	46.8
2/2	1.13	33.1
4/0+	1.10	25.0
4/2+	1.11	26.3
4/4	1.07	39.3
6/0+	1.07	*
6/2+	1.04	*

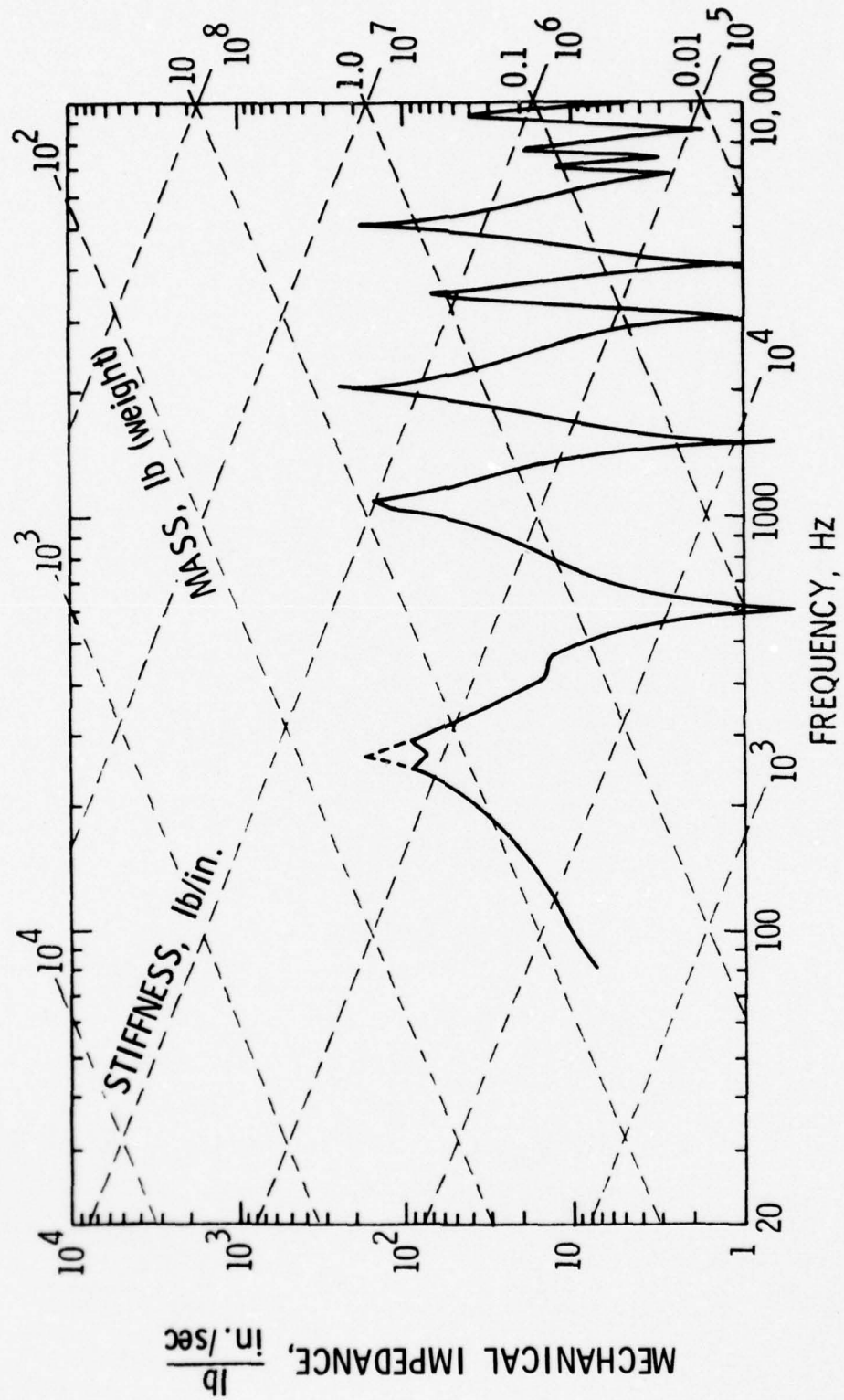

Figure 12. Measured driving-point impedance at the center of a uniform aluminum plate (12.0 x 12.0 x 0.375 in.) coated with a 0.25 in. thick layer of Epoxy 10 damping treatment.

TABLE VI

FREQUENCY SHIFT FACTOR $D_{f,a}$ AND LOSS FACTOR RATIO $R_{g,a}$ FOR THE AIR-LOADED SQUARE PLATE COATED WITH EPOXY 10 DAMPING COMPOUND

p/q	Frequency Shift Factor $D_{f,a}$	Loss Factor Ratio $R_{g,a}$ (dB)
2/0+	0.92	29.0
2/2	0.93	17.9
4/0+	0.93	11.5
4/2+	0.93	12.3
4/4	0.93	24.2
6/0+	0.93	32.3
6/2+	0.88	*

5.2 Water-Loaded Case

Several special forms of the Frequency Shift Factor and the Loss Factor Ratio are now defined. A Frequency Shift Factor, denoted $D_{f,w}$, is defined as the ratio of the measured resonant frequency of a coated plate, water-loaded, to the corresponding measured resonant frequency of the reference plate, water-loaded. This definition is similar to that defined for $D_{f,a}$ (Section 5.1) except that the plate loading condition is that of water instead of air. Another Frequency Shift Factor, denoted $D_{f,w-a}$, is defined as the ratio of the measured resonant frequency of a plate, water-loaded, to the corresponding measured resonant frequency of the same plate, air-loaded. As defined, $D_{f,w-a}$ provides a measure of the shift in the resonant frequencies caused by the change in the plate loading conditions. A Loss Factor Ratio is defined in decibels as 20 $\log_{10}$ of the ratio of the measured loss factor of a particular resonance of a coated plate, water-loaded, to the measured loss factor of the corresponding resonance of the reference plate, water-loaded. Thus, $R_{g,w}$ is defined in a manner similar to that of $R_{g,a}$ (Section 5.1) except for a difference in the plate loading conditions. Another Loss Factor Ratio is defined as 20 $\log_{10}$ of the ratio of the measured loss factor of a particular resonance of a plate, water-loaded, to the measured loss factor of the corresponding resonance of the same plate, air-loaded. Denoted $R_{g,w-a}$, this Loss Factor Ratio indicates in decibels the change in the loss factor of a plate due to changes in the loading condition.

A. Reference Plate. The measured driving-point impedance of the centrally excited reference plate, water-loaded on one side, is plotted in Figure 13. Comparison of the mode shapes measured for this case with those of the same plate, air-loaded, show no change in the nodal patterns, indicating that its modal characteristics are not affected by the water loading. Listed in Table VII are the Frequency Shift Factors $D_{f,w-a}$ and Loss Factor Ratios $R_{g,w-a}$ for each resonance. Note that the Frequency Shift Factors listed are less than unity, indicating a shift downward in frequency of the resonances. This downward shift is a result of the addition of an inertia term caused by the water loading. The Loss Factor Ratios listed in Table VII are positive, a result of the increased radiation of energy caused by the strong fluid-structure coupling.

B. Coated Plates. In Figures 14 through 17 are plotted the measured driving-point impedances of the LD400, GP-1, VE and Epoxy 10 coated plates, water-loaded. Listed in Tables VIII through XI are the Frequency Shift Factors $D_{f,w}$ and $D_{f,w-a}$ and the Loss Factor Ratios $R_{g,w}$ and $R_{g,w-a}$ for these four coated plates. The Frequency Shift Factors $D_{f,w}$ tabulated in these tables are approximately equal to the values of $D_{f,a}$ listed in Tables III through VI, indicating that the relative shift in the resonance frequencies caused by the attachment of the coatings has not been changed by the change in the fluid loading condition. Water loading of the reference plate was seen to increase the modal mass resulting in a downward shift in frequency of the resonances. Approximately equal downward shifts in the resonant frequencies of the

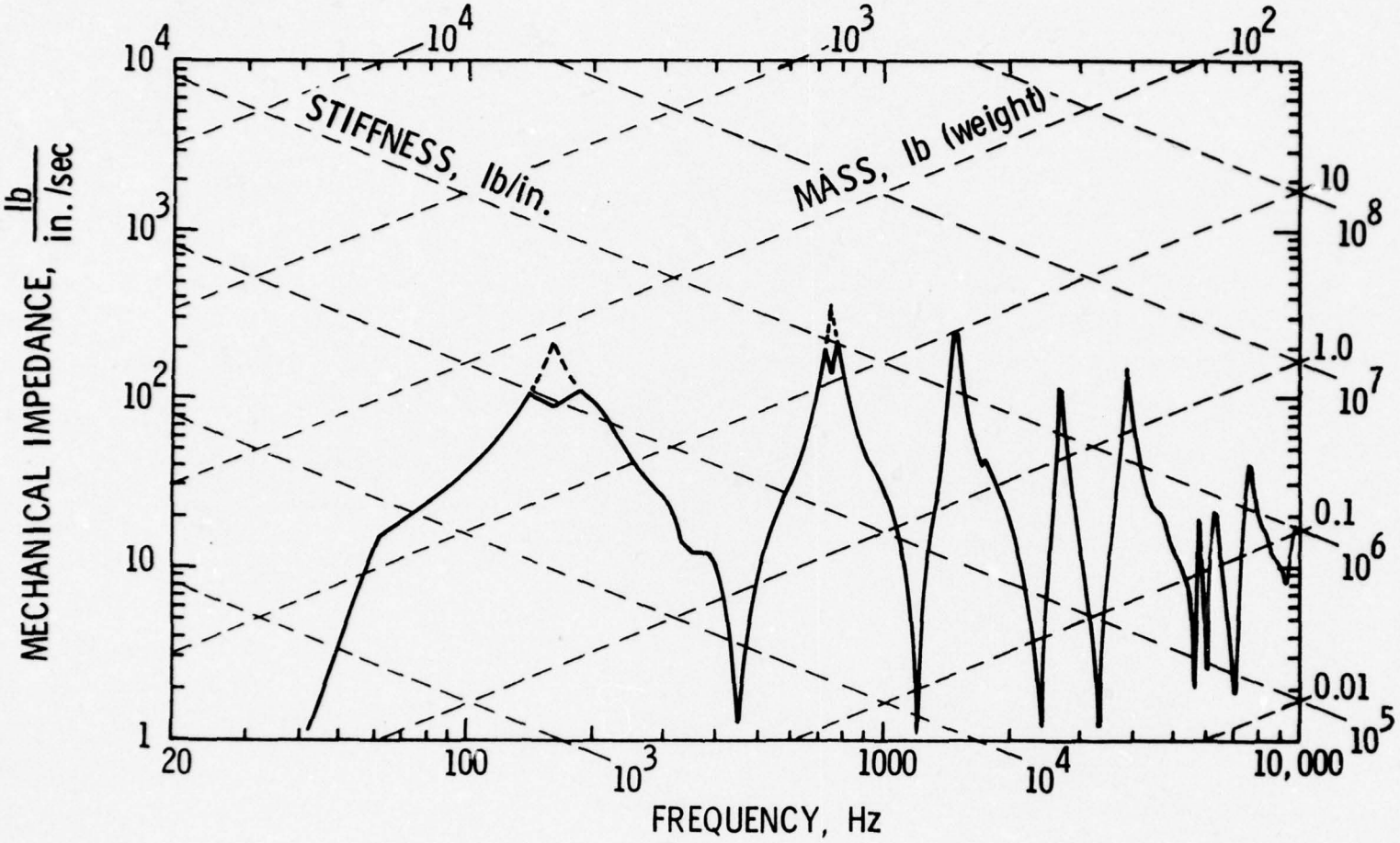

Figure 13. Measured driving-point impedance at the center of the square (12.0 x 12.0 x 0.375 in.) aluminum reference plate water-loaded on one side.

TABLE VII

FREQUENCY SHIFT FACTOR $D_{f,w-a}$ AND LOSS FACTOR RATIO $R_{g,w-a}$ FOR THE WATER-LOADED REFERENCE PLATE

p/q	Frequency Shift Factor $D_{f,w-a}$	Loss Factor Ratio $R_{g,w-a}$ (dB)
2/0+	0.68	15.4
2/2	0.74	2.2
4/0+	0.75	3.1
4/2+	0.78	10.0
4/4	0.81	15.3
6/0+	0.80	20.8
6/2+	0.77	*

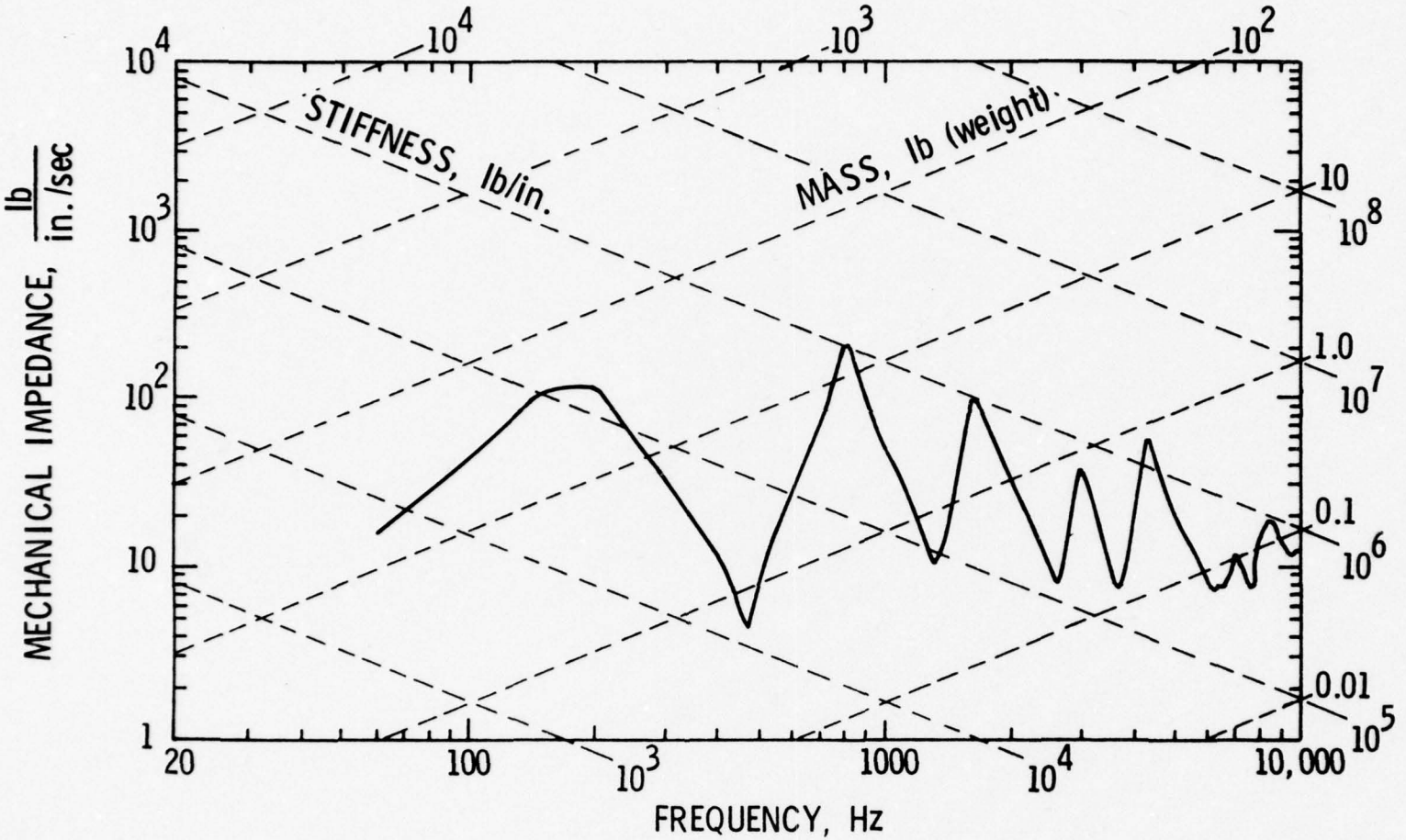

Figure 14. Measured driving-point impedance at the center of a uniform aluminum plate (12.0 x 12.0 x 0.375 in.) water-loaded on one side and coated with a 0.25 in. thick layer of LD400 damping treatment.

TABLE VIII

FREQUENCY SHIFT FACTORS AND LOSS FACTOR RATIOS

FOR THE WATER-LOADED SQUARE PLATE

COATED WITH LD400 DAMPING TILE

p\q	Frequency Shift Factor $D_{f,w}$	Frequency Shift Factor $D_{f,w-a}$	Loss Factor Ratio $R_{g,w}$ (dB)	Loss Factor Ratio $R_{g,w-a}$ (dB)
2/0+	1.11	0.75	34.7	-0.04
2/2	1.17	0.83	34.3	-1.2
4/0+	1.15	0.82	24.5	-1.6
4/2+	1.14	0.84	17.7	-1.3
4/4	1.14	0.87	*	*
6/0+	1.11	0.85	*	*
6/2+	1.13	0.85	24.2	4.7

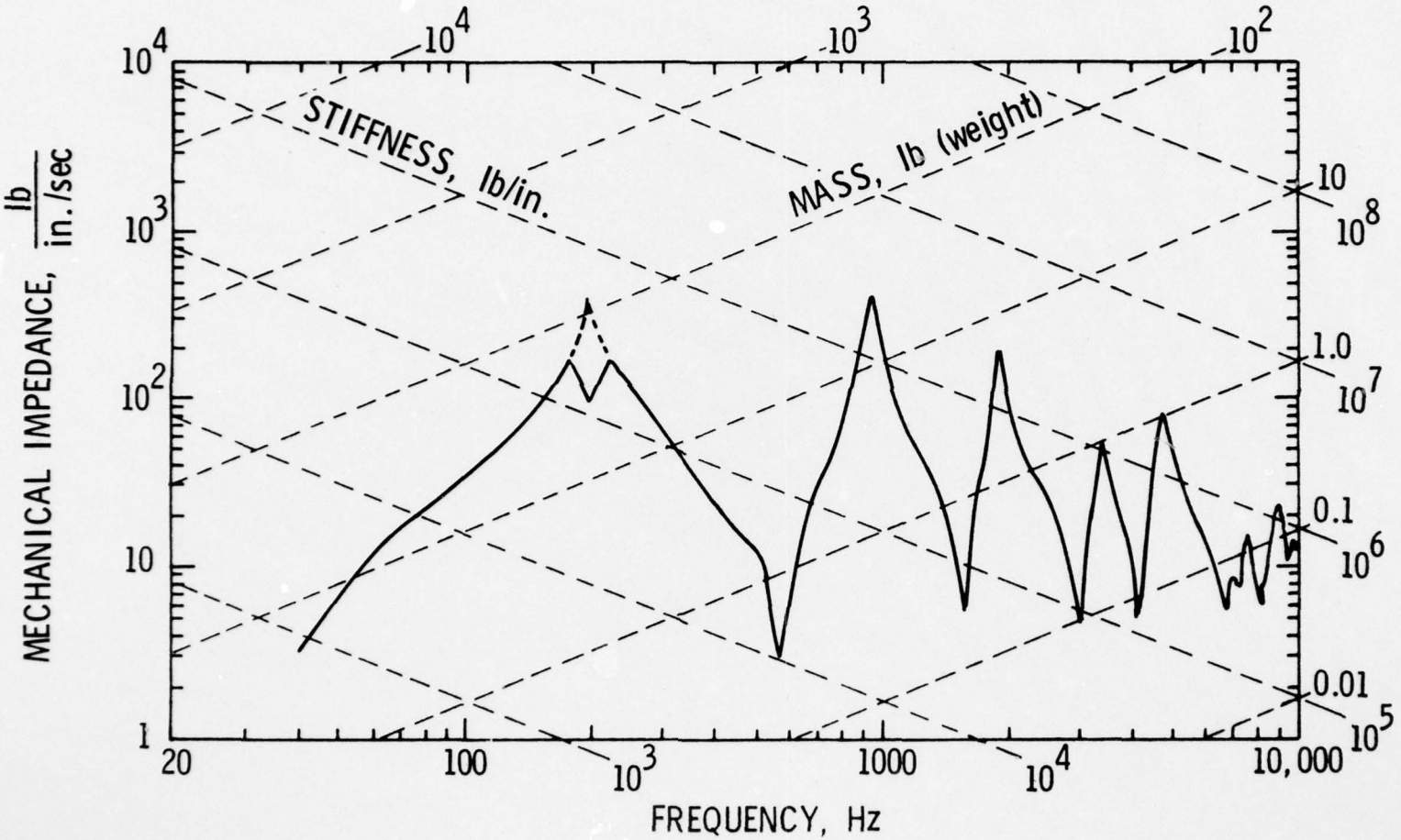

Figure 15. Measured driving-point impedance at the center of a uniform aluminum plate (12.0 x 12.0 x 0.375 in.) water-loaded on one side and coated with a 0.25 in. thick layer of GP-1 damping treatment.

TABLE IX

FREQUENCY SHIFT FACTORS AND LOSS FACTOR RATIOS

FOR THE WATER-LOADED SQUARE PLATE

COATED WITH GP-1 DAMPING COMPOUND

p\q	Frequency Shift Factor $D_{f,w}$	Frequency Shift Factor $D_{f,w-a}$	Loss Factor Ratio $R_{g,w}$ (dB)	Loss Factor Ratio $R_{g,w-a}$ (dB)
2/0+	1.23	0.71	29.7	0.8
2/2	1.28	0.77	29.0	1.4
4/0+	1.23	0.78	20.1	0.7
4/2+	1.21	0.80	14.5	2.9
4/4	1.16	0.83	*	*
6/0+	1.16	0.83	*	*
6/2+	1.18	0.83	17.0	*

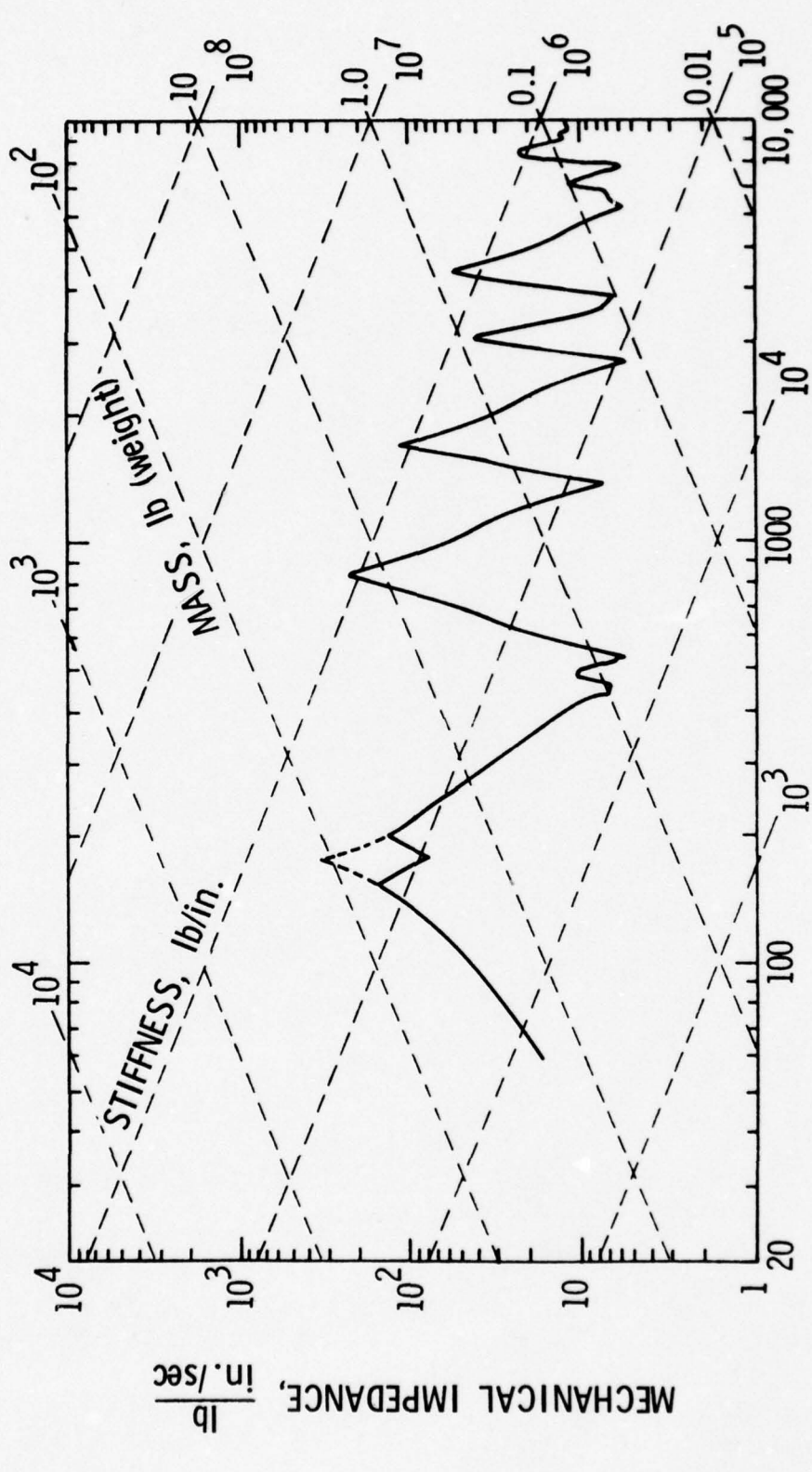

Figure 16. Measured driving-point impedance at the center of a uniform aluminum plate (12.0 x 12.0 x 0.375 in.) water-loaded on one side and coated with a 0.25 in. thick layer of Embossed Foam Damping Sheet (VE).

TABLE X

FREQUENCY SHIFT FACTORS AND LOSS FACTOR RATIOS

FOR THE WATER-LOADED SQUARE PLATE

COATED WITH VE DAMPING TILE

p\q	Frequency Shift Factor $D_{f,w}$	Frequency Shift Factor $D_{f,w-a}$	Loss Factor Ratio $R_{g,w}$ (dB)	Loss Factor Ratio $R_{g,w-a}$ (dB)
2/0+	1.16	0.73	31.3	-0.1
2/2	1.19	0.78	31.0	0.1
4/0+	1.16	0.79	22.4	0.5
4/2+	1.15	0.81	20.8	4.6
4/4	1.12	0.85	*	*
6/0+	1.12	0.83	*	*
6/2+	1.11	0.82	19.2	2.8

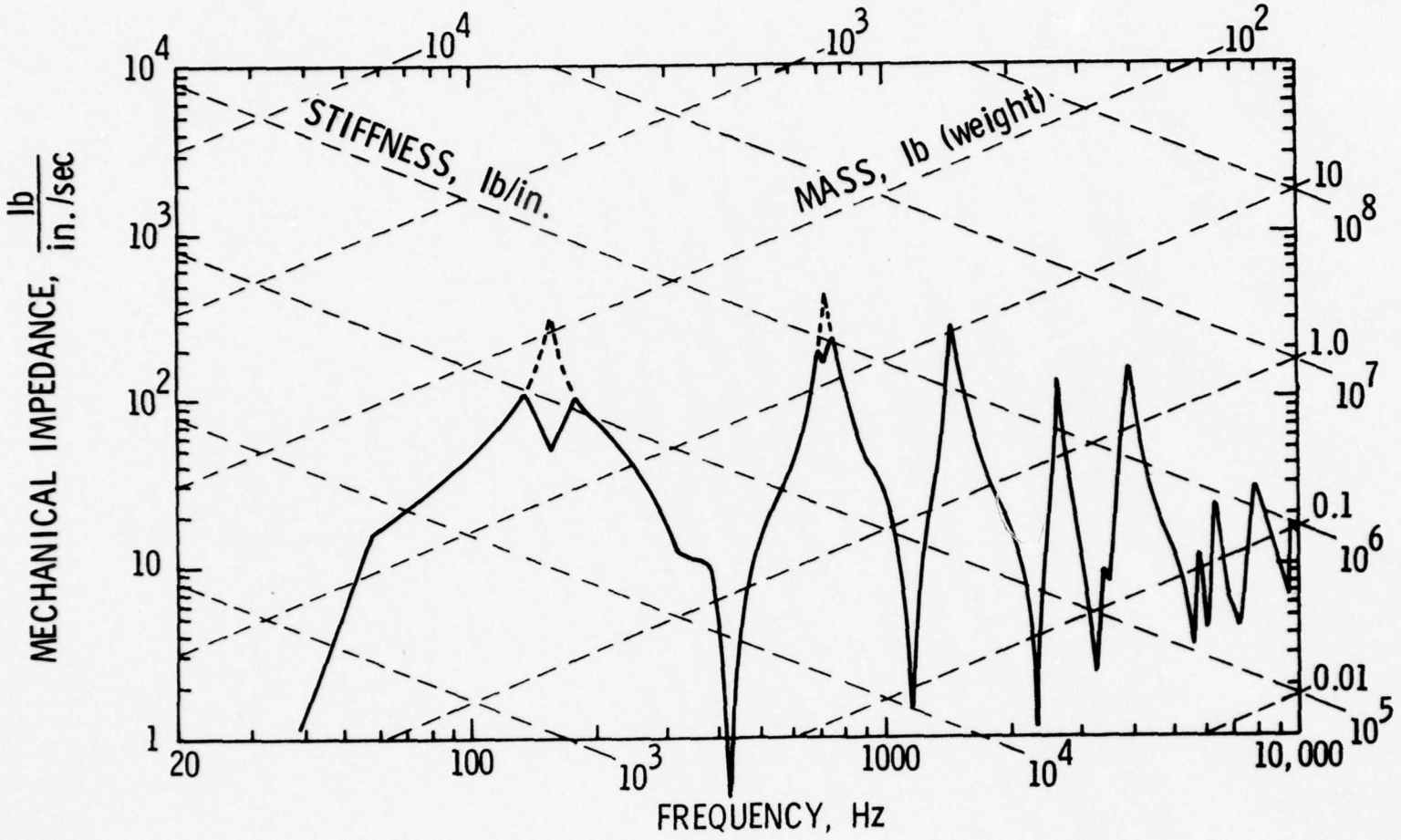

Figure 17. Measured driving-point impedance at the center of a uniform aluminum plate (12.0 x 12.0 x 0.375 in.) water-loaded on one side and coated with a 0.25 in. thick layer of Epoxy 10 damping treatment.

TABLE XI

FREQUENCY SHIFT FACTORS AND LOSS FACTOR RATIOS

FOR THE WATER-LOADED SQUARE PLATE

COATED WITH EPOXY 10 DAMPING COMPOUND

p\q	Frequency Shift Factor $D_{f,w}$	Frequency Shift Factor $D_{f,w-a}$	Loss Factor Ratio $R_{g,w}$ (dB)	Loss Factor Ratio $R_{g,w-a}$ (dB)
2/0+	0.96	0.71	15.2	1.6
2/2	0.96	0.77	15.0	-0.6
4/0+	0.96	0.78	7.8	-0.6
4/2+	0.96	0.80	6.5	4.2
4/4	0.96	0.83	13.7	4.8
6/0+	0.96	0.82	14.7	3.2
6/2+	0.96	0.85	10.1	3.0

coated plates are indicated by the Frequency Shift Factors $D_{f,w-a}$ tabulated in these tables. From this, it is evident that the per unit increase in the modal masses of each plate, coated and uncoated, caused by the water loading of one side of each, is equivalent.

5.3 Sound Radiation

Figure 18 shows the spectrum of the sound level measured in the test tank for the water-loaded reference plate. The shaker was driven with wide band random noise (0^{+}-10 kHz). Absolute units have not been used since only qualitative results were of interest. Levels below 500 Hz have been obscured by the ambient noise level in the tank and, therefore, are not shown in this and all subsequent sound level spectra. The measurement hydrophone was situated 6 ft. directly below the plate in the test tank, such that it was located in the direct sound field of the plate. The pronounced peaks in the spectrum correspond in frequency to maximum force input to the plate, which generally occurs at the antiresonances. Normalization of this spectrum by the force input to the plate did not provide further insight into the sound radiation characteristics, and normalization by the power input to the plate was not possible with the experimental apparatus.

Shown in Figures 19 through 22 are the spectrum of the sound levels measured in the test tank for the water-loaded LD400, GP-1, VE, and Epoxy 10 coated plates. These plates were driven in the same manner as that of the reference plate, using wide band random noise to drive the shaker. Experimental parameters (preamplifier gains, drive signal, processor controls) were kept the same during the measurement of the sound level for each plate in order to allow a qualitative comparison of the spectra. The LD400 and VE coatings have caused the most significant reductions in the sound level, resulting in as much as 20 dB attenuation over certain frequency bands. Sound levels between 5,000 Hz and 10,000 Hz have been reduced 10-15 dB by the use of these treatments.

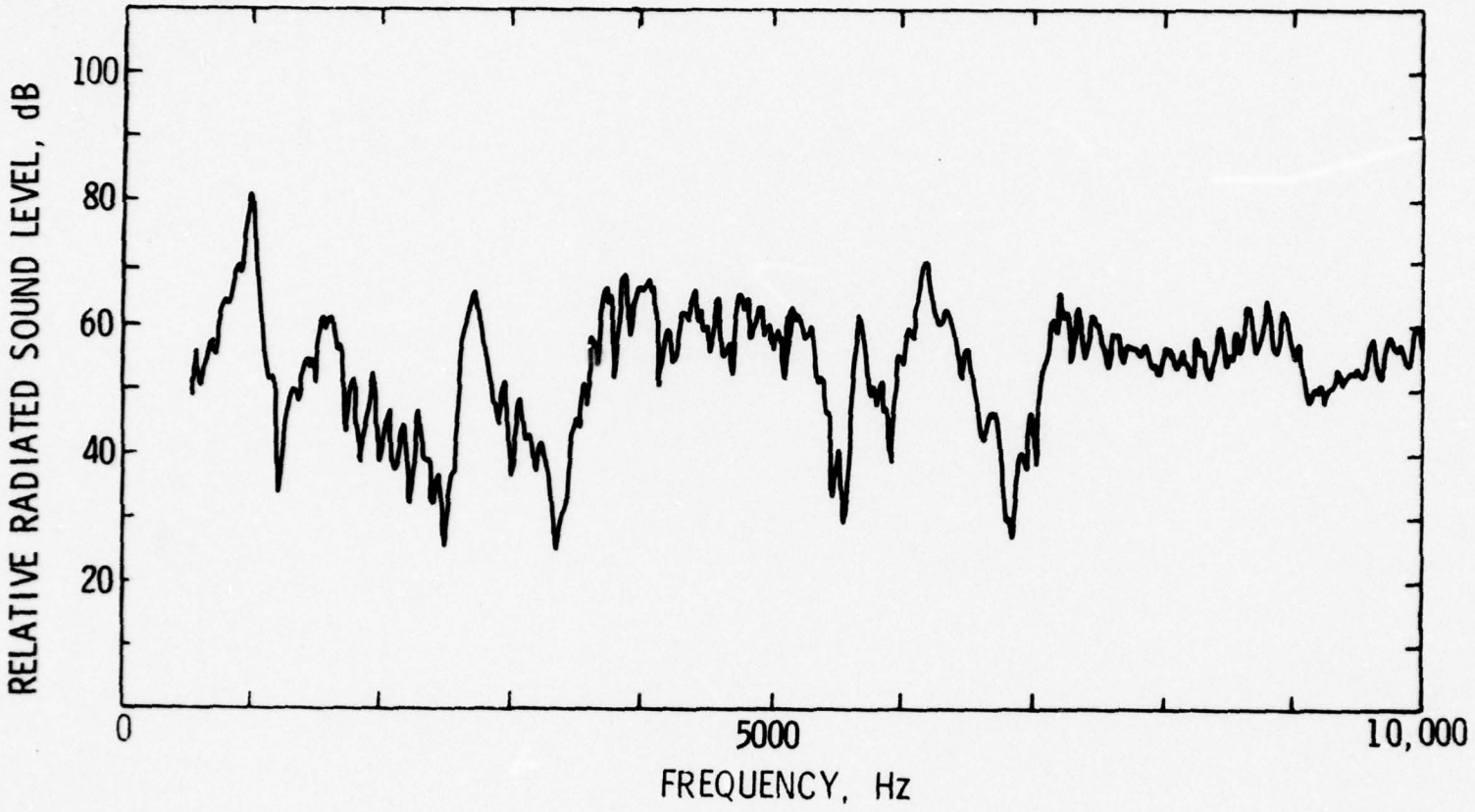

Figure 18. Spectrum of sound level in test tank, 6 ft. below center of water-loaded, aluminum reference plate.

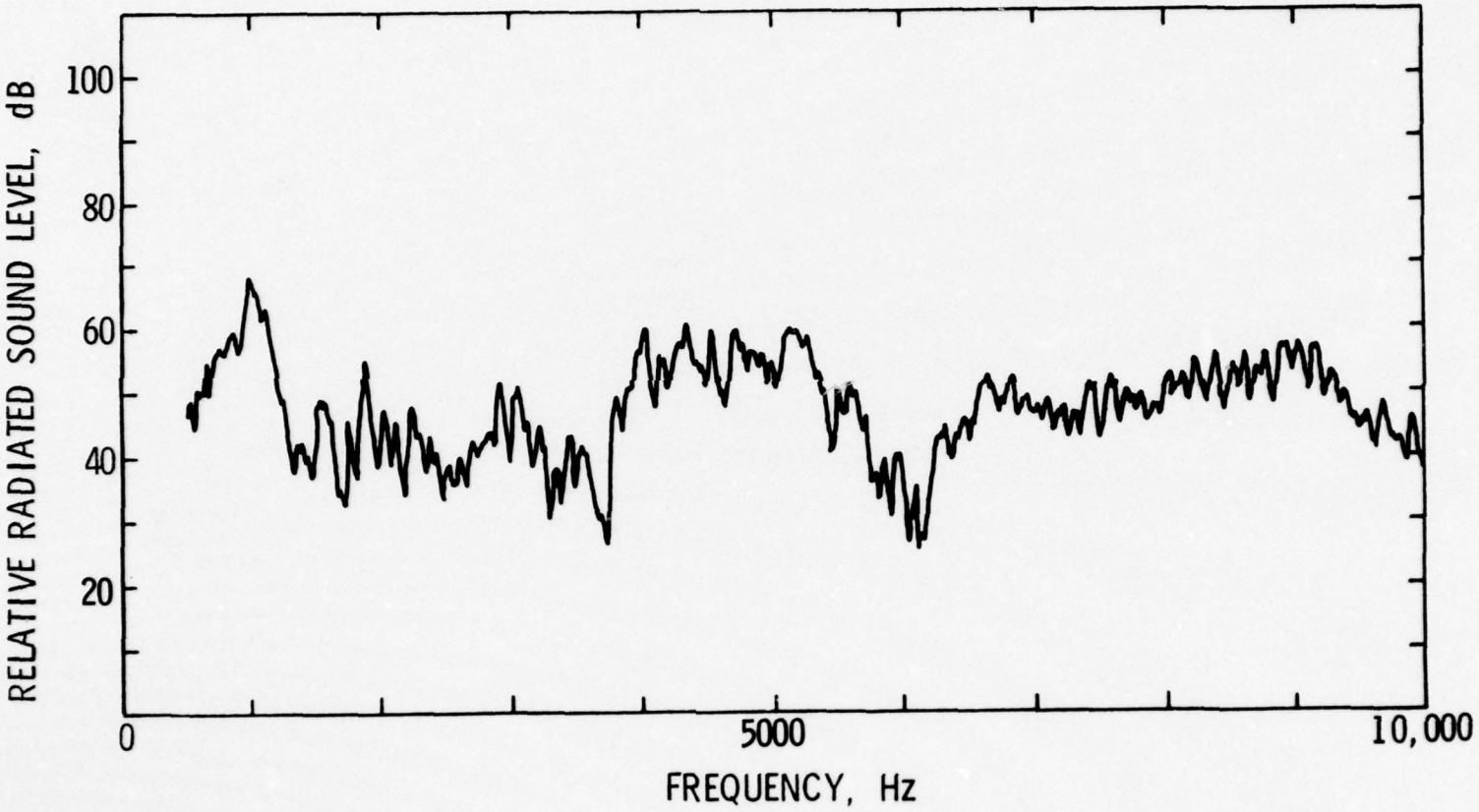

Figure 19. Spectrum of sound level in test tank, 6 ft. below center of water-loaded, aluminum plate (12.0 x 12.0 x 0.375 in.) coated with a 0.25 in. thick layer of LD400 damping treatment.

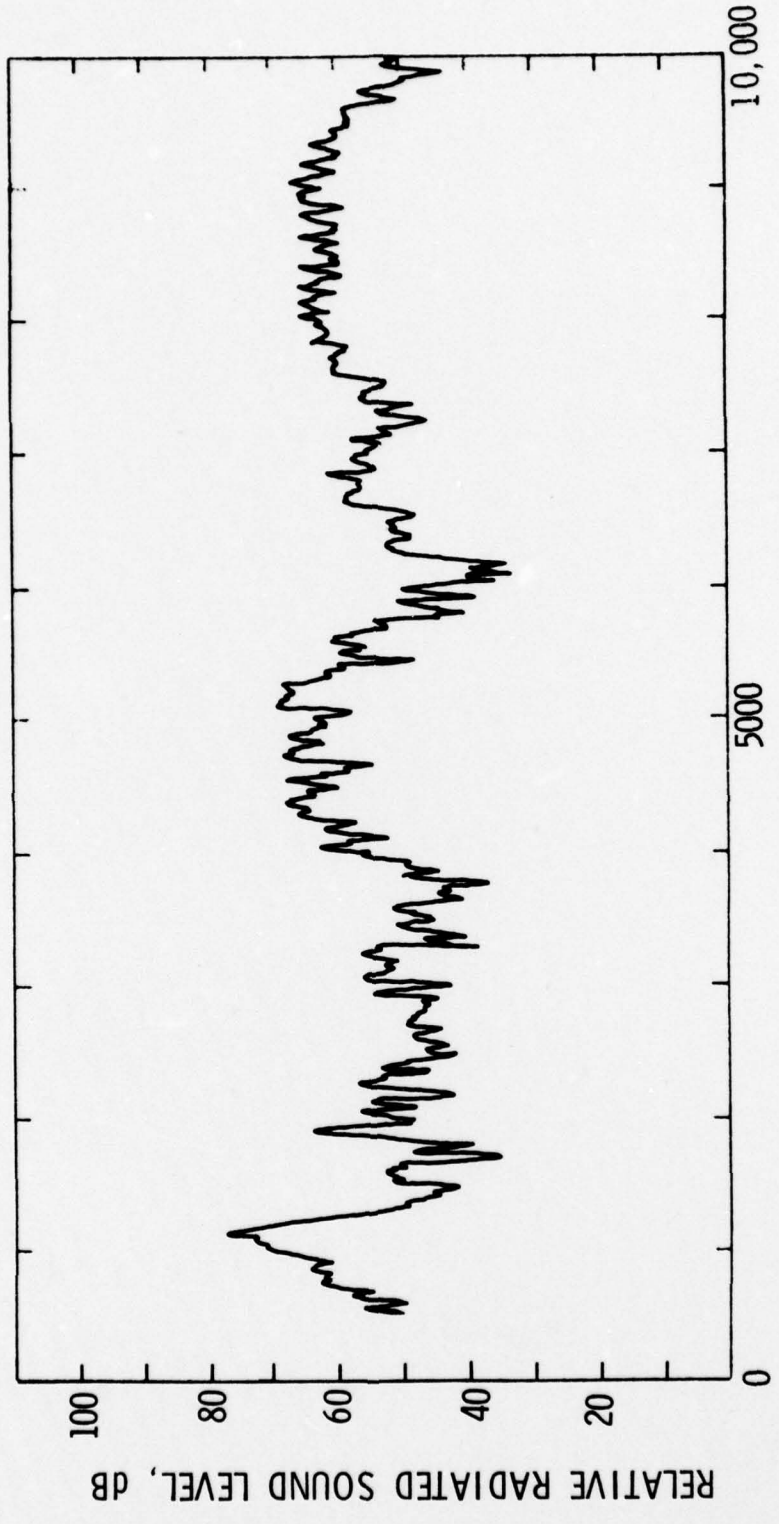

Figure 20. Spectrum of sound level in test tank, 6 ft. below center of water-loaded, aluminum plate (12.0 x 12.0 x 0.375 in.) coated with a 0.25 in. thick layer of GP-1 damping treatment.

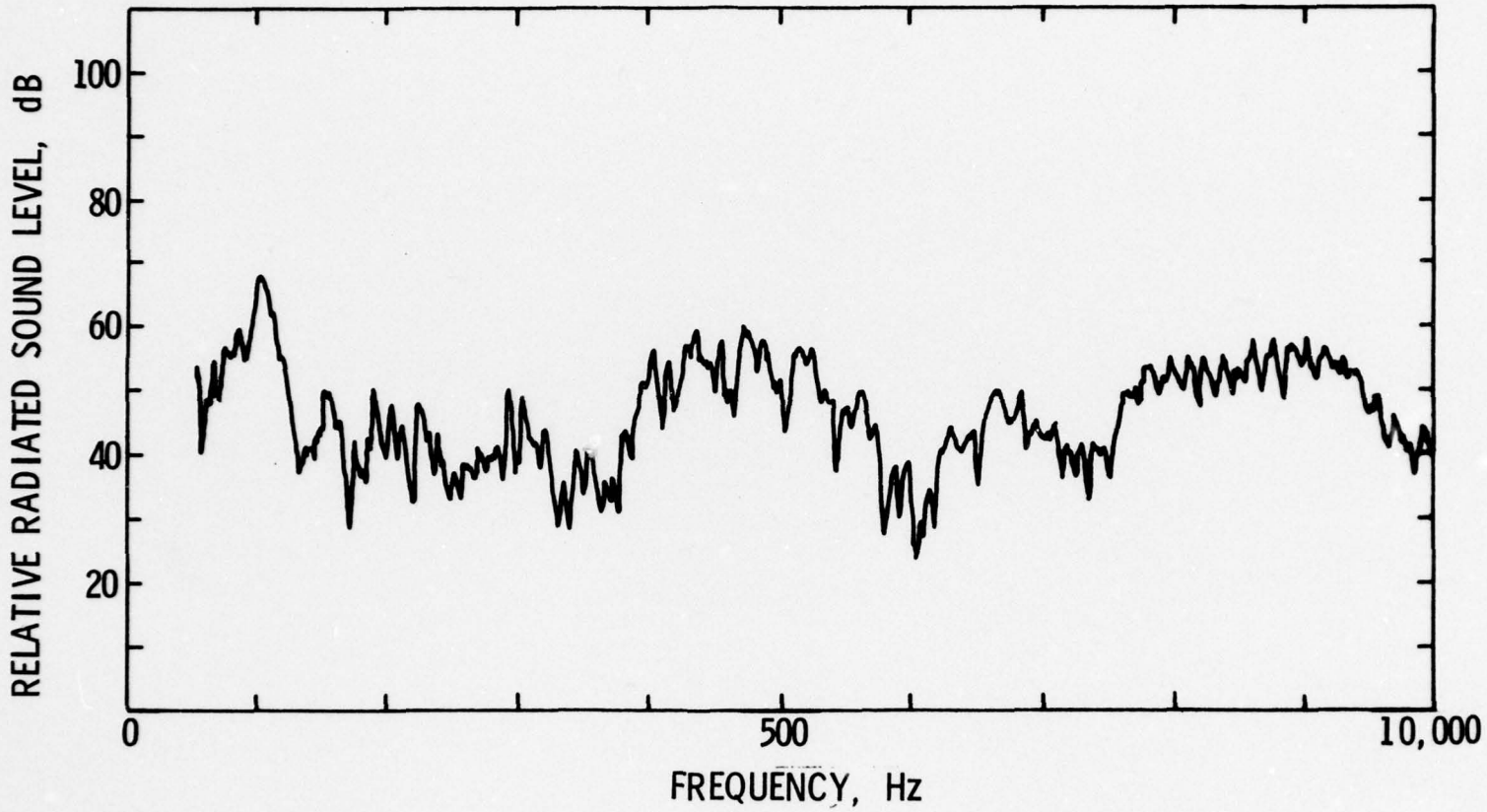

Figure 21. Spectrum of sound level in test tank, 6 ft. below center of water-loaded, aluminum plate (12.0 x 12.0 x 0.375 in.) coated with a 0.25 in. thick layer of Embossed Foam Damping Sheet (VE).

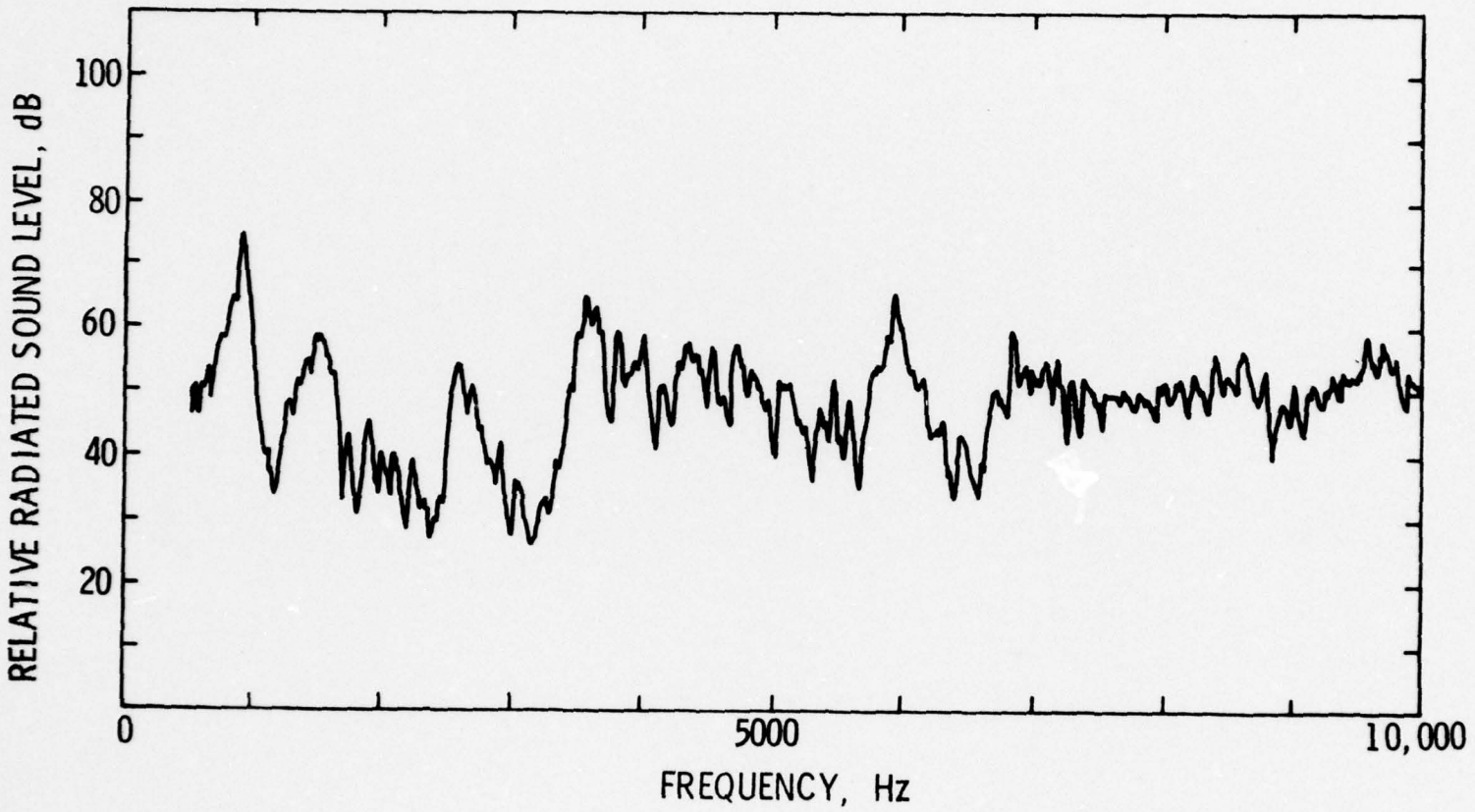

Figure 22. Spectrum of sound level in test tank, 6 ft. below center of water-loaded, aluminum plate (12.0 x 12.0 x 0.375 in.) coated with a 0.25 in. thick layer of Epoxy 10 damping treatment.

CHAPTER VI

SUMMARY AND CONCLUSIONS

6.1 Summary

A comparison study was undertaken to evaluate the effectiveness of several commercially available damping treatments in the reduction of the transverse vibrations of fluid-loaded plates. Considered were center-driven, square, aluminum plates which were unconstrained along all edges. Damping treatments were attached to the upper surface of these plates in accordance with manufacturers' specifications. The plates were subjected to two types of fluid loading; air loading on both sides, and water loading on one side.

The driving-point impedances of these treated plates were measured over the extended frequency range of up to 10 kHz using digital signal processing techniques. From these, the resonant frequencies and loss factors were determined and compared with those of an uncoated reference plate. Frequency shift factors and loss factor ratios were introduced. These provided a measure of the effects of the coatings and the change in the fluid loading conditions on the modal characteristics of the plates. Measurements of the sound level in an acoustic water tank were made for each plate and compared in order to gain insight into the effects of the treatments on the sound radiation into the test tank by the water-loaded plates.

Very favorable agreement between experimental results and theory is

found for the case of the centrally driven, uncoated, reference plate, air-loaded. Measured resonant frequencies are seen to correspond well to theoretical values determined using the methods of Warburton (1954). Mode shapes measured for the reference plate coincide with those observed by Waller (1939), providing information about the mode numbers of each plate resonance excited.

Loss factors derived from measured impedance data indicate that LD400 and Embossed Foam Damping Sheet (VE) are the most effective treatments tested in reducing the plate vibrations. These two treatments have, for all plate resonances excited, increased the loss factors by at least 25 dB as compared to that of the uncoated reference plate. Interestingly, all but one of the treatments tested have the effect of increasing the modal stiffness of the plates more than the modal mass. As a result, the resonances of the plates coated with these treatments have shifted upwards in frequency from that of the reference plate. Only the addition of the Epoxy 10 results in a greater increase in the modal mass and a downward shift in frequency of the resonances.

Water loading of one side of the test plates results in no change in their modal characteristics. However, an additional inertia term, introduced by the heavy fluid loading, causes a shift downward in frequency of the resonances. Also, the strong fluid-structure interaction increases the loss factors of each plate mode by as much as 20 dB. However, this increase is not as pronounced as that caused by the more effective damping treatments (LD400 and VE).

Addition of the more effective treatments (LD400 and VE) to the

water-loaded plate increases the loss factors of the modes excited by at least 15 dB as compared to that of the water-loaded, reference plate. Moreover, the overall change in the loss factors from the air-loaded to the water-loaded case is no more than $\pm$5 dB, indicating that the effects of these treatments overshadows any water loading effects.

Comparison of the spectra of the sound levels measured in the test tank for each water-loaded plate indicate that the LD400 and Embossed Foam Damping Sheet (VE) are the most effective of the treatments tested in reducing sound radiation, causing as much as 20 dB attenuation over certain frequency bands and 10 dB to 15 dB attenuation over most frequencies between 5-10 kHz.

6.2 Conclusions

Tile type damping treatments, such as LD400 and Embossed Foam Damping Sheet (VE), have proven to be the most effective of the treatments tested in reducing the transverse vibrations and sound radiation of centrally excited, free, square plates. The increase in the loss factors of each plate mode excited due to these treatments was found to be greater than any increase due to the water loading. Thus, the addition of these treatments to the internal portions of a submerged body should increase the loss factors of each transverse mode excited. The increase of the loss factors should result in greater internal energy dissipation, which in turn should reduce the energy available for transfer into the ambient medium as acoustic sound waves.

Knowledge of a treatment's effectiveness in an air-loaded

environment has provided sufficient information to rate its effectiveness in a water-loaded environment. This is evident when it is noted that, of the treatments tested here, the most effective ones, LD400 and VE, caused the greatest increase in the loss factors of both the air-loaded and water-loaded plates. Thus, the treatments which were most effective in reducing the vibrations of air-loaded plates were found to be the most effective in the water-loaded mode.

BIBLIOGRAPHY

1. American National Standard Method for the Measurement of Mechanical Mobility, Part 1: Basic Definitions and Transducers, 7th draft, January, 1978.

2. Bendat, J. S. and Piersol, A. G., Measurement and Analysis of Random Data, John Wiley and Sons, Inc., New York, 1966.

3. Blake, W. K., "The Radiation from Free-Free Beams in Air and in Water," J. Sound and Vib., 33, 427-450, (1974).

4. Cremer, L. and Heckl, M., Structure-Borne Sound, trans. Ungar, E. E., Springer-Verlag, New York, 1973.

5. Davies, H. G., "Low Frequency Random Excitation of Water-Loaded Rectangular Plates," J. Sound and Vib., 15, 107-126, (1971).

6. Engblom, J. J. and Nelson, R. B., "In-Fluid Response of Complex Structures With Application to Orthotropic Spheres," J. Sound and Vib., 49, 1-8, (1976).

7. Ewins, D. J., "Measurement and Application of Mechanical Impedance Data, Part 1. Introduction and Ground Rules," J. Soc. Environ. Eng., 14, No. 4, 3-13, (1975).

8. Ewins, D. J., "Measurement and Application of Mechanical Impedance Data, Part 2. Measurement Techniques," J. Soc. Environ. Eng., 15, No. 1, 23-33, (1976).

9. Ewins, D. J., "Measurement and Application of Mechanical Impedance Data, Part 3. Interpretation and Application of Measured Data," J. Soc. Environ. Eng., 15, No. 2, 7-17, (1976).

10. Firth, D., "Acoustic Vibration of Structures in Liquids," Shock and Vib. Digest, 9, No. 9, 3-77, (1977).

11. Goodman, L. E., "Material Damping and Slip Damping," in Shock and Vibration Handbook, 2nd ed., Ch. 36, eds. Harris, C. M. and Crede, C. E., McGraw-Hill, New York, (1976).

12. Halvorsen, W. G. and Brown, D. L., "Impulse Technique for Structural Frequency Response Testing," Sound and Vib., 11, No. 11, 8-21, (1977).

13. Junger, M. C. and Feit, D., Sound, Structures, and Their Interaction, The MIT Press, Cambridge, Massachusetts, 1972.

14. Kennedy, C. C. and Pancu, C. D. P., "Use of Vectors in Vibration Measurement and Analysis," J. Aeronautical Sciences, 14, 603-625, (1947).

15. Kerlin, R. L., "Transverse Vibration of Uniform and Nonuniform, Internally Damped Cantilever Beams," Ph.D. thesis, The Pennsylvania State University, 1972.

16. Klosterman, A. L., "On the Experimental Determination and Use of Modal Representations of Dynamic Characteristics," Ph.D. thesis, University of Cincinnati, 1971.

17. Klosterman, A. L., "Determination of Dynamic Information By Use of Vector Components of Vibration," M.S. thesis, University of Cincinnati, 1968.

18. Lang, G. F., "Understanding Vibration Measurements," Sound and Vib., 10, No. 3, 26-37, (1976).

19. Leibowitz, R. C., "Vibroacoustic Response of Turbulence Excited Thin Rectangular Finite Plates in Heavy and Light Fluid Media," J. Sound and Vib., 40, 441-495, (1975).

20. Ochs, J. B., "Transmissibility Across Simply Supported, Rectangular, Thin Plates With Loading Masses or Ribs," M.S. thesis, The Pennsylvania State University, 1975.

21. Plunkett, R., "Vibration Control by Applied Damping Treatments," in Shock and Vibration Handbook, 2nd ed., Ch. 37, eds. Harris, C. M. and Crede, C. E., McGraw-Hill, New York, (1976).

22. Skudrzyk, E. J., "Vibrations of a System With a Finite or an Infinite Number of Resonances," J. Acoust. Soc. Am., 30, 1140-1152, (1958).

23. Spectral Dynamics Corporation, "Measuring Structural Transfer Functions in Real Time," Application Manual DSP-008, San Diego, California, (1976).

24. Spectral Dynamics Corporation, "The Measurement of Structural Transfer Functions and Mechanical Impedance," Technical Publication M-3, San Diego, Califorinia, (1976).

25. Snowdon, J. C., Vibration and Shock in Damped Mechanical Systems, John Wiley and Sons, Inc., New York, 1968.

26. Waller, M. D., "Vibrations of Free Square Plates: Part I. Normal Vibrating Modes," Proc. Phys. Soc., 51, 831-844, (1939).

27. Warburton, G. B., "The Vibration of Rectangular Plates," Inst. Mech. Eng., 168, 371-383, (1954).

28. Ungar, E. E., "Damping of Panels," in Noise and Vibration Control, Ch. 14, ed. Beranek, L. L., McGraw-Hill, New York, (1971).

APPENDIX A

Mass Cancellation

The Wilcoxon Z820 impedance head used during the experimental phase of this investigation contains internally a force gage and an accelerometer. These are mounted along the driving axis of the shaker and measure the acceleration and input force at the drive point of the plate.

The force measured by the force gage is typically slightly different from the actual force applied to the plate by the shaker. This is because some of the indicated force is 'used' to accelerate the small mass between the measuring crystals of the force gage and the plate. This added mass, termed the end effective mass or the mass below the force gage, consists, in part, of the mass of the driving platform of the gage and any other material, such as the stud, used to attach the plate to the shaker. This end effective mass may not be negligible when compared with the effective modal mass of a mode of vibration of the plate. It must therefore be compensated for.

During the experimental phase of this investigation, electrical compensation was used to correct for the effects of the end effective mass. This required that a portion of the acceleration signal be subtracted from the force signal. Analog subtraction was performed by the mass cancellation system, which is seen in Figure 23. This system consisted of two Ithaco preamplifiers and a mass cancellation circuit, comprised of three operational amplifiers with associated circuitry.

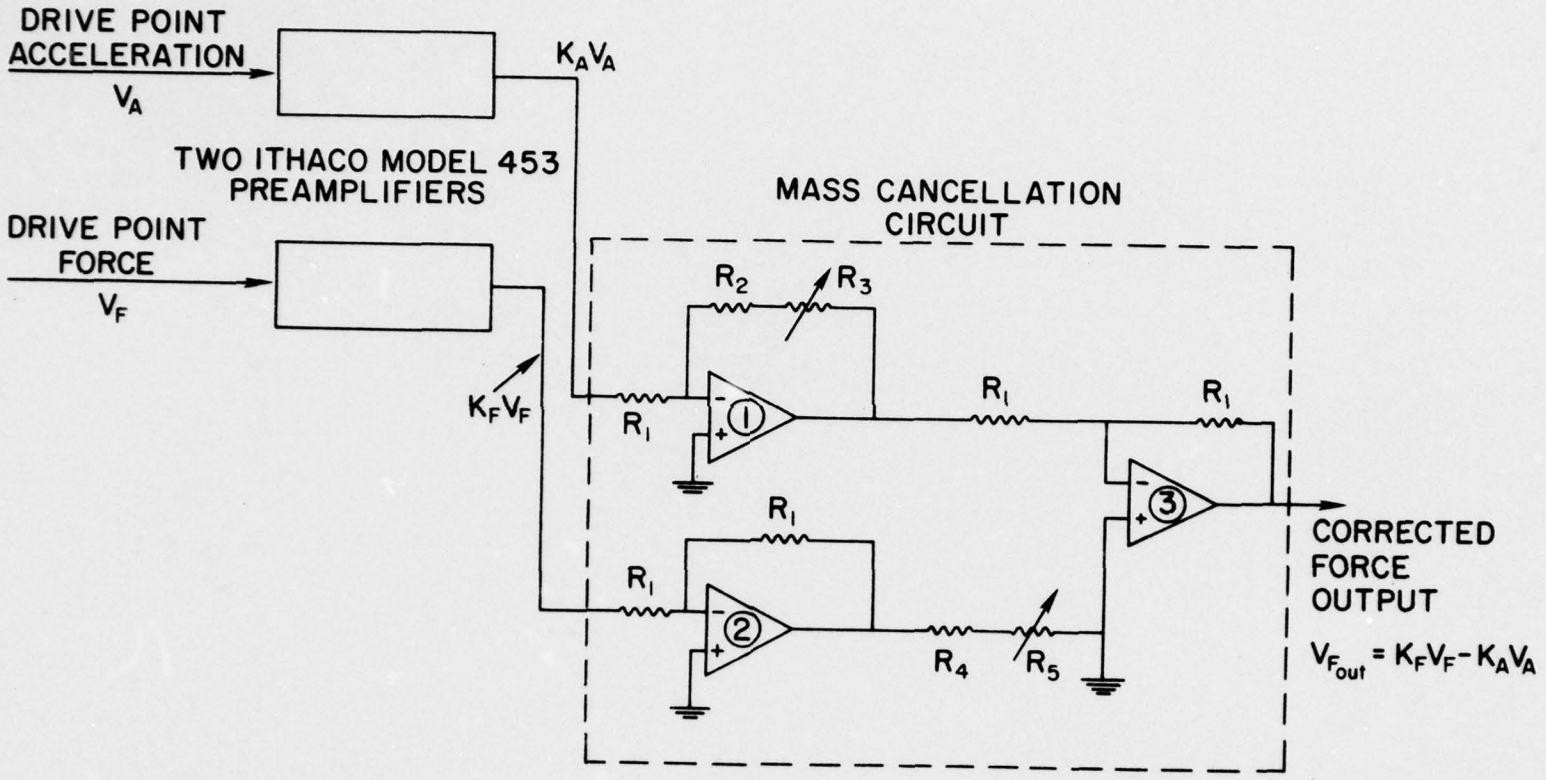

Figure 23. Mass Cancellation System.

The AC acceleration and force voltage signals were amplified by the preamplifiers and fed into the inputs of operational amplifiers 1 and 2, respectively. The acceleration signal was multiplied by a weighting factor, $K_A = \frac{R_2 + R_3}{R_1}$ in amplifier 1. The gain of amplifier 2 was unity. Both signals were then fed into amplifier 3, which is a unity gain difference amplifier. This subtracted the weighted acceleration signal from the force signal, resulting in an output which was the corrected force signal. Unity gain in amplifier 3 was assured by varying R_5 prior to calibration.

Calibration of this circuit was accomplished by driving the impedance head with only the attachment stud connected. Under this loading condition, the only force indicated by the force gage was that required to drive the end effective mass. The weighting factor of the acceleration signal was varied by changing the gains of the Ithaco preamplifier and operational amplifier 1 until a minimum force signal was obtained.

DISTRIBUTION

Commander (NSEA 09G32)
Naval Sea Systems Command
Department of the Navy
Washington, DC 20362 — Copies 1 and 2

Commander (NSEA 0342)
Naval Sea Systems Command
Department of the Navy
Washington, DC 20362 — Copies 3 and 4

Defense Documentation Center
5010 Duke Street
Cameron Station
Alexandria, VA 22314 — Copies 5 through 16